

NOTE TO USERS

This reproduction is the best copy available.

UMI[®]

A NOVEL SELF-POWERED SUPPLY FOR GCT GATE DRIVERS

by

Weiqian Hu

Bachelor of Engineering, Shenyang University of Technology, China, 1996

A thesis

presented to Ryerson University

in partial fulfillment of the

requirements for the degree of

Master of Applied Science

in the Program of

Electrical and Computer Engineering

Toronto, Ontario, Canada, 2006

©(Weiqian Hu) 2006

**PROPERTY OF
RYERSON UNIVERSITY LIBRARY**

UMI Number: EC53499

INFORMATION TO USERS

The quality of this reproduction is dependent upon the quality of the copy submitted. Broken or indistinct print, colored or poor quality illustrations and photographs, print bleed-through, substandard margins, and improper alignment can adversely affect reproduction.

In the unlikely event that the author did not send a complete manuscript and there are missing pages, these will be noted. Also, if unauthorized copyright material had to be removed, a note will indicate the deletion.



UMI Microform EC53499
Copyright 2009 by ProQuest LLC
All rights reserved. This microform edition is protected against
unauthorized copying under Title 17, United States Code.

ProQuest LLC
789 East Eisenhower Parkway
P.O. Box 1346
Ann Arbor, MI 48106-1346

AUTHOR'S DECLARATION

I hereby declare that I am the sole author of this thesis.

I authorize Ryerson University to lend this thesis to other institutions or individuals for the purpose of scholarly research.

I further authorize Ryerson University to reproduce this thesis by photocopying or by other means, in total or in part, at the request of other institutions or individuals for the purpose of scholar research.

BORROWER'S PAGE

Ryerson University requires the signatures of all persons using or photocopying this thesis.

Please sign below, and give address and date.

[illegible]

A Novel Self-powered Supply for GCT Gate Drivers

Master of Applied Science

2006

Weiqian Hu

Electrical and Computer Engineering

Ryerson University, Canada

ABSTRACT

This thesis is devoted to the development of a novel self-powered supply (SPS) for the gate driver of integrated Gate Commutated Thyristors (GCT). In commercial GCT power supplies, a high-voltage isolation transformer is an indispensable device. Since the GCT devices are normally for high-power converters operating at a voltage level of $2.3KV$ to $13.8KV$, the high-voltage isolation transformer is expensive in cost and bulky in size. The SPS proposed in this thesis transfers energy from GCT snubber circuits and generates a regulated dc supply for the GCT gate driver. Since the snubber circuit is at the same potential as the GCT device, the insulation level of the self-powered supply is reduced from a few thousand volts to a couple of hundred volts, leading to a significant reduction in cost and size.

In this thesis, the configuration of the proposed SPS is presented, and its operating principle is elaborated. The strategy for maximizing the SPS output power is analyzed. It is demonstrated that the SPS can provide a regulated output up to $60W$ for most commercial GCT gate drivers. The performance of the SPS is verified by experiments on a $60W$ laboratory prototype.

ACKNOWLEDGEMENTS

I would like to express my deep gratitude to my supervisor, Professor Bin Wu, for his foremost support and help during my graduate studies at Ryerson University. His valuable advice and guidance has greatly enhanced my academic knowledge, scientific inspiration and practical skills.

I am grateful to Professor Richard Cheung, Professor David Xu, Dr. Yunwei Li, and all fellow students at LEDAR for their useful discussions on my research. I sincerely thank Mr. Albert Qiu, for his detailed review and comments on my thesis. My appreciation also goes to Mr. Jim Koch for his help in preparing the PCB boards, and Mr. Angelo Bortus for his assistance in experiments at Rockwell Automation Canada.

I also wish to share my achievements with my families and my wife Connie Wu. I am very grateful for my dear wife's understanding and support.

TABLE OF CONTENTS

| | |
|---|----|
| CHAPTER 1 INTRODUCTION..... | 1 |
| 1.1 Power Supplies for Gate Drivers | 3 |
| 1.1.1 Commercial Power Supply for Gate Drivers..... | 3 |
| 1.1.2 Self-powered Supplies (SPS)..... | 4 |
| 1.2 Motivation and Objectives | 9 |
| 1.3 Thesis Organization..... | 11 |
| CHAPTER 2 PRINCIPLE OF SELF-POWERED SUPPLY FOR GCT GATE DRIVER..... | 13 |
| 2.1 Introduction | 13 |
| 2.2 Technical Requirements and Configuration of the Proposed SPS..... | 13 |
| 2.2.1 Technical Requirements..... | 14 |
| 2.2.2 SPS Configuration..... | 16 |
| 2.2.3 Converter 1 for Energy Storage..... | 17 |
| 2.2.4 Converter 2 for Regulated DC Output Voltage..... | 22 |
| 2.2.5 Design Guidance for C_e and SPS Start-up Process | 27 |
| 2.3 Conclusion..... | 29 |
| CHAPTER 3 MODELING, SIMULATION AND ANALYSIS | 31 |
| 3.1 Introduction | 31 |
| 3.2 Modeling of SPS and GCT Gate Driver..... | 31 |
| 3.2.1 Modeling of Self-Powered Supply (SPS)..... | 31 |
| 3.2.2 Modeling of GCT Gate Driver | 33 |
| 3.2.3 SPS PSIM Model..... | 38 |
| 3.3 Simulation for Maximum Output Power | 39 |
| 3.4 Simulation of Startup Process..... | 43 |
| 3.5 Summary | 45 |
| CHAPTER 4 EXPERIMENTS | 47 |
| 4.1 Verification of Simulation Model..... | 47 |
| 4.2 SPS Prototype..... | 49 |
| 4.3 Experiments on SPS | 50 |
| 4.3.1 Constant dc Input Voltage..... | 52 |
| 4.3.2 Input Voltage with High Fluctuation | 55 |
| 4.3.3 Verification of Hysteresis Band of the MOSFET Controller..... | 57 |
| 4.4 Summary | 59 |

| | |
|--|----|
| CHAPTER 5 CONCLUSIONS..... | 61 |
| APPENDIX..... | 65 |
| A. Typical Parameters of A Medium-voltage Current Source Rectifier | 65 |
| B. Specifications for Commercial GCT Gate Drivers | 66 |
| C. GCT Gate Driver | 66 |
| D. Schematic of the Self-powered Supply Prototype | 68 |
| REFERENCES..... | 71 |

LIST OF FIGURES

| | | |
|-----------|--|----|
| Fig. 1-1 | GCT block diagram. | 2 |
| Fig. 1-2 | PWM current source rectifier (CSR). | 2 |
| Fig. 1-3 | Block diagram of the commercial gate driver power supply for GCT devices..... | 4 |
| Fig. 1-4 | A self-powered supply circuit for the GTO gate driver..... | 5 |
| Fig. 1-5 | A self-powered supply circuit for the SCR gate driver. | 7 |
| Fig. 1-6 | A self-powered gate driver for an anti-parallel thyristor pair..... | 9 |
| Fig. 2-1 | PWM Current Source Rectifier (CSR) with six self-powered supplies. | 14 |
| Fig. 2-2 | Circuit diagram of the self-powered supply for GCT gate drivers. | 17 |
| Fig. 2-3 | Typical voltage and current waveforms for GCT device and capacitors. | 19 |
| Fig. 2-4 | Charging process with $v_{GCT} > 0$ | 20 |
| Fig. 2-5 | Charging process for $v_{GCT} < 0$ | 21 |
| Fig. 2-6 | Circuit diagram of Converter 2..... | 22 |
| Fig. 2-7 | Waveforms of the flyback converter operating in a discontinuous mode. | 23 |
| Fig. 2-8 | Flyback converter waveforms – continuous mode. | 26 |
| Fig. 2-9 | V_{start} , V_{min} , v_{CE} and MOSFET operation status. | 29 |
| Fig. 3-1 | Circuit diagram of the SPS for the GCT gate driver. | 33 |
| Fig. 3-2 | GCT turn-on and turn-off gate current waveform..... | 36 |
| Fig. 3-3 | Simplified GCT gate driver circuit. | 37 |
| Fig. 3-4 | Simulated waveforms for the GCT gate driver. | 38 |
| Fig. 3-5 | Simulation Model for SPS and GCT gate driver..... | 39 |
| Fig. 3-6 | Determination of SPS maximum output power. | 40 |
| Fig. 3-7 | $P_{O,max}$ versus C_e | 41 |
| Fig. 3-8 | $P_{O,max}$ versus C_s | 42 |
| Fig. 3-9 | $P_{O,max}$ versus V_{LL} | 43 |
| Fig. 3-11 | t_2 versus C_e | 45 |
| Fig. 4-1 | Experimental waveforms for v_{GCT} and i_{GD} | 48 |
| Fig. 4-2 | GCT gate driver and SPS Prototype. | 50 |
| Fig. 4-3 | Simplified SPS circuit diagram..... | 51 |
| Fig. 4-4 | Waveforms of the SPS on no load condition..... | 52 |
| Fig. 4-5 | Waveforms of the SPS operating in a discontinuous mode..... | 54 |
| Fig. 4-6 | Waveforms of the SPS operating in a continuous mode..... | 55 |
| Fig. 4-7 | Highly fluctuated input voltage and stable SPS output voltage..... | 56 |
| Fig. 4-8 | Discontinuous and continuous mode waveforms of the SPS with a fluctuated input voltage. | 56 |
| Fig. 4-9 | Waveforms for the hysteresis band of the MOSFET controller..... | 57 |
| Fig. A-1 | Circuit diagram of GCT gate driver..... | 67 |
| Fig. A-2 | Block diagram of SPS and GCT gate driver..... | 68 |
| Fig. A-3 | Schematic of the self-powered supply Prototype..... | 68 |

CHAPTER 1

INTRODUCTION

The high power converters with power rating from 0.4MW to 40MW at the medium voltage level of 2.3KV to 13.8KV are widely applied in industry [1], such as medium voltage (MV) drives, static reactive compensators (STATCOM), and dynamic voltage restorers (DVR). High power MV drives are increasingly used in petrochemical, mining, steel and metals, transportation, and other industries to enhance energy efficiency, increase productivity and improve product quality [1]. STATCOMs can be utilized to regulate voltage, control power factor, and stabilize power flow [2]. DVRs are commonly applied to correct voltage sags, swells, and unexpected load changes, so as to maintain the voltage within acceptable tolerances [3].

In high power converters, Gate Turn Off (GTO) thyristors had been widely used until the advents of high-power Insulated Gate Bipolar Transistors (IGBTs) and integrated Gate Commutated Thyristors (GCTs) in the late 1990s [4,5]. These new generation switching devices have rapidly entered the main areas of high-power electronics due to their superior switching characteristics, reduced power losses, and ease of gate control [1]. Currently, the voltage and current rating of IGBT devices can reach 6.6kV/0.6KA or 1.7KV/3.6KA, while the ratings of GCTs can be up to 6KV/6KA. Thus GCTs are more suitable for higher power applications.

The GCT device is essentially a high power GTO integrated with a specially designed gate driver. The gate driver has an extremely low gate inductance, which leads to a great improvement of GCT turn-off capability over conventional GTOs [6,7]. Fig. 1-1 shows the block diagram of a GCT device. The gate driver, which is normally powered by a 20V dc supply, converts the gate signals generated by the digital controller into required GCT gating currents.

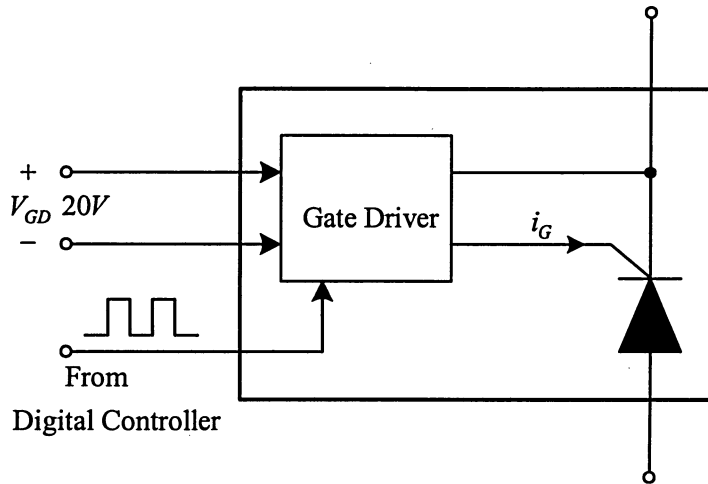


Fig. 1-1 GCT block diagram.

Fig.1-2 shows a typical topology of GCT based Current Source Rectifiers (CSR) commonly used in medium voltage drives as a front-end converter [1]. The line inductance L_s and filter capacitor C_f form a low pass filter to attenuate harmonics generated by the CSR. The dc choke L_d is used to smooth the dc current.

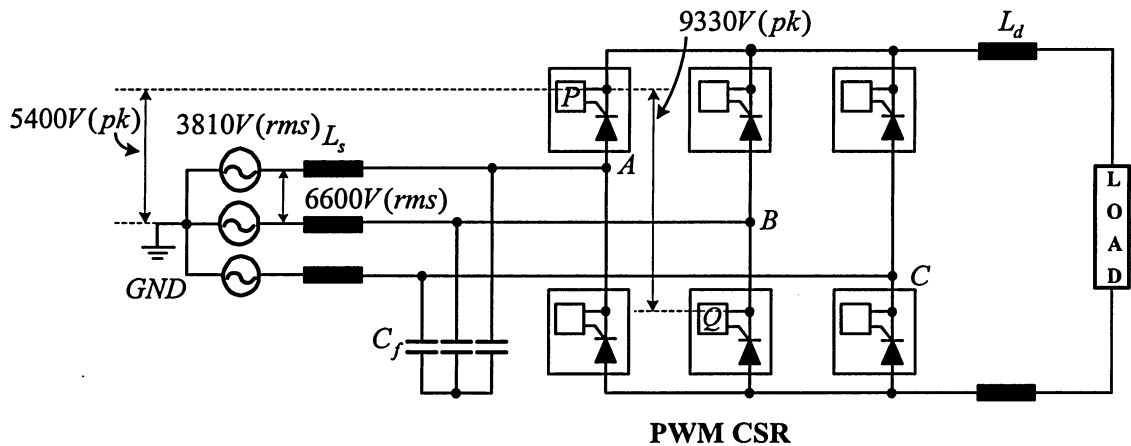


Fig. 1-2 PWM current source rectifier (CSR).

Since the gate driver is connected to the cathode and gate of the GCT device, the gate driver and its power supply are at the same potential of the GCT. For example, in a $6600V$ system, the voltage of gate driver P with respect to ground GND is $5400V(peak)$, and the voltage between gate driver P and gate driver Q is $9330V(peak)$. As a result, high voltage isolation for the power supply is required [8-11].

To fulfill the aforementioned isolation requirement, separate power supplies insulated by isolation transformers are normally used for GCT gate drivers. These isolation transformers are quite expensive and bulky, which cause an increase in the manufacturing cost and the physical size of the power converters.

In order to decrease the system cost and size, several self-powered supply (SPS) techniques were proposed in literature [12-14]. The main purpose of these techniques is to use energy from power converter or snubber circuits of switching devices to power the gate drivers such that the isolation transformers can be eliminated for system cost reduction.

1.1 Power Supplies for Gate Drivers

There are two types of power supplies for switching device gate drivers, the commercial isolation transformer based power supplies and the self-powered supplies. In this section, these two types of power supplies are introduced, discussed, and compared.

1.1.1 Commercial Power Supply for Gate Drivers

A commercial power supply for a switching device gate driver is normally composed of an isolation transformer, a rectifier, and a dc-dc converter. Fig. 1-3 shows the typical block diagram

of this type of power. Depending on GCT's current capability, the power rating of the GCT gate driver is normally in the range of $10W$ to $60W$. The isolation transformer converts a utility ac to a lower ac voltage, which is then converted into a dc voltage by the rectifier. This dc voltage may vary with the utility voltage and/or the load conditions, and thus it is further stabilized to power the gate driver by a dc-dc converter.

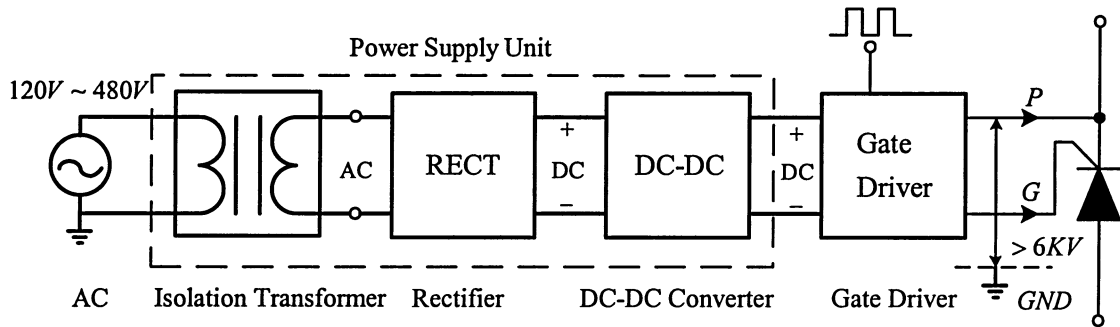


Fig. 1-3 Block diagram of the commercial gate driver power supply for GCT devices.

Another important function of the isolation transformer is to provide isolation between utility power supply and the gate driver. Since the voltage between the switching device and the ground of the utility power supply can be a few thousands volts in MV applications, the isolation transformer must be specially designed and manufactured. Hence the cost of such a transformer is high and its physical size is large.

1.1.2 Self-powered Supplies (SPS)

To reduce the cost of gate driver supplies, several self-powered supply (SPS) techniques were proposed in literature. The purpose of these techniques is to utilize the energy of power circuits or snubber circuits to power the gate drivers, instead of using energy transferred from the utility power supply via isolation transformers.

1) Self-powered supply for GTO gate drivers

Fig. 1-4 shows a self-powered supply circuit for the GTO gate driver [12]. The supply circuit consists of a snubber capacitor C_1 , a snubber diode D_1 , an inductor L_1 , a power disposing circuit (including a diode D_2 , a capacitor C_2 and a resistor R_1), an electric energy storage capacitor C_3 and a diode D_3 . The main purpose of the supply circuit is to convert the energy stored in the magnetic field of inductor L_1 into the electric energy of the capacitor to power the GTO gate driver.

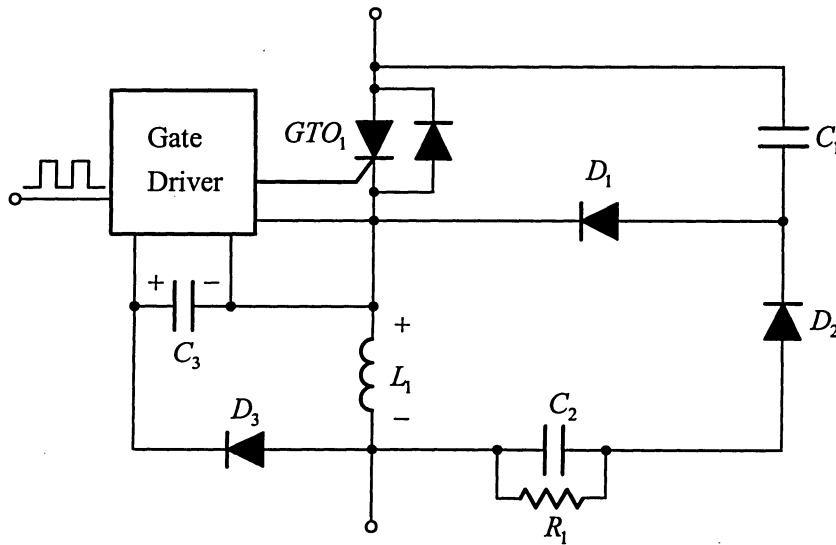


Fig. 1-4 A self-powered supply circuit for the GTO gate driver.

The operating principle of this design is based on the Lenz's law of the inductor L_1 . When the current of inductor L_1 increases, a positive voltage appears across the inductor, and the field energy of the inductor increases. The diode D_3 is reverse-biased so that the electric energy stored in the capacitor C_3 cannot be released into L_1 . Once the inductor current decreases, the

voltage across the inductor will become negative. Then the diodes D_2 and D_3 will conduct, and the magnetic field energy stored in the inductor L_1 will be transferred into the electric energy and stored in capacitors C_2 and C_3 . The resistor R_1 dissipates the energy stored in C_2 to smooth the dc voltage. In this method, the electric energy in capacitor C_3 supplies the GTO gate driver so that the isolation transformer is no longer needed.

However, this design has its limitations and cannot be used for GCT applications. The reasons are given as follows.

- High cost of the inductors. Each of the self-powered supply requires an inductor in series with the GTO device. Since this inductor carries the same current as that in GTO, its size is large and cost is high. This is especially true for those converters with two or more switches in series. The use of the inductors makes this scheme impractical, especially for GCTs, where no inductors are normally required.
- No voltage regulation at the SPS output. The dc voltage accuracy does not fulfill the requirement of the GCT gate driver. In this method, the dc voltage is maintained by the capacitor C_2 . Thus the voltage ripple and variation may be larger than the requirement (typically $\pm 0.5V$) of the power supply for GCT gate drivers.

2) Self-powered Supply for SCR Gate Drivers

Fig. 1-5 shows a self-powered supply circuit for the SCR gate driver [13]. The SPS is composed of a current limiting resistor R_1 , a zener diode Z_1 , an energy storage capacitor C_1 ,

and a voltage regulator U_1 . It collects energy from the snubber circuit (R_s , D_s , and C_s) to power the SCR gate driver.

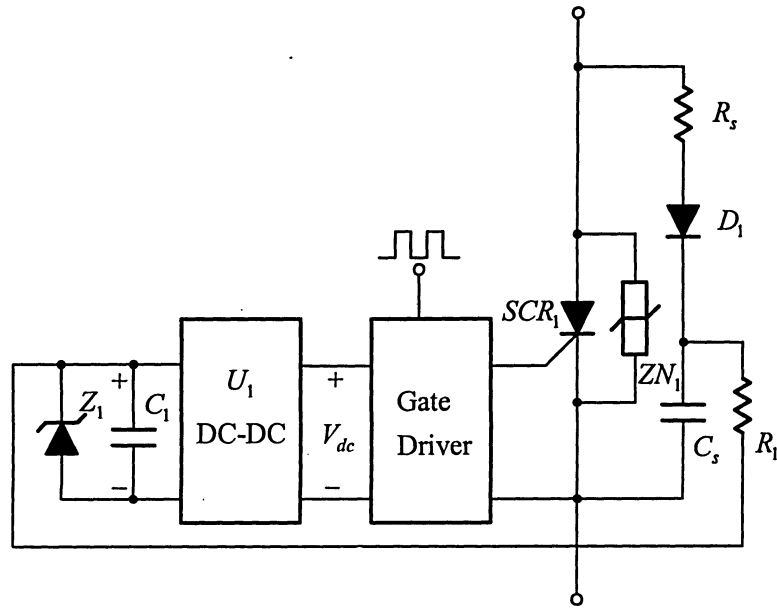


Fig. 1-5 A self-powered supply circuit for the SCR gate driver.

The energy storage capacitor C_1 absorbs energy from the snubber network through the current limiting resistor R_1 . The voltage across C_1 is clamped by zener diode Z_1 . The voltage regulator circuit U_1 converts the voltage across C_1 into a regulated voltage V_{dc} to supply the SCR gate driver. The surge absorber ZN_1 is applied to clamp the voltage across the SCR_1 to a safe range.

This scheme features a regulated dc supply for the SCR gate drivers. However, there are a couple of drawbacks associated with this design. One drawback is that the surge absorber ZN_1 is not practical for MV applications due to large amount of energy consumed on the absorber. Another limitation is that this SPS can only be used for SCR gate driver, which requires only

small amount of power, typically a few watts. Therefore, this method cannot be applied to the GCT gate driver.

3) Self-powered Supply for Anti-parallel SCR Pairs

Fig. 1-6 shows a self-powered gate driver for a pair of anti-parallel SCRs [14]. This method collects the energy from the snubber capacitor to power its gate driver. The SPS is composed of an RC snubber circuit (R_s and C_s) and two energy storage capacitors (C_1 and C_2). The energy can be transferred to C_1 and C_2 when the SCRs are turned off. The stored energy in C_1 and C_2 supplies gate drivers $GD1$ and $GD2$, respectively. Thus the circuit operates in a self-powered manner. To limit the voltage on C_1 and C_2 , two voltage clamping circuits are used, which consist of resistors R_1 and R_2 , zener diodes Z_1 and Z_2 , and thyristors T_1 and T_2 , respectively. For example, when the voltage across C_1 reaches the breakdown voltage of the zener diode Z_1 , the diode will be reverse-conducting, and the thyristor T_1 will be fired. Consequently, the current will be diverted from C_1 to T_1 , and the diode D_{1R} will be reverse-biased, preventing C_1 from discharging through T_1 . The clamping circuit for capacitor C_2 operates in a similar manner, and therefore is not discussed here.

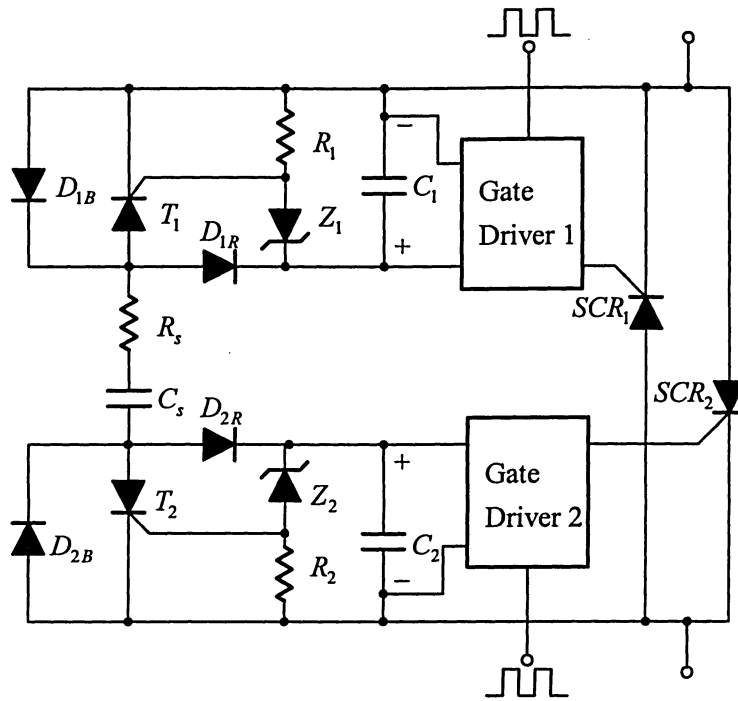


Fig. 1-6 A self-powered gate driver for an anti-parallel thyristor pair.

However, this SPS technology is not suitable for GCT gate drivers. The GCT not only requires power to turn on, but also demands a large amount of energy to switch off. Since this method is designed for SCR pairs, the energy used to fire the SCRs is not enough for GCT gatings. Further, the dc voltage of the power supply is not regulated to meet the requirement of GCT gate drivers.

1.2 Motivation and Objectives

With the advent of integrated Gate Commutated Thyristors (GCT), high power converters operating at medium voltage levels (2.3KV to 13.8KV) are increasingly employed in industry. Each GCT device normally requires a specially designed power supply for its gate driver. Commercial GCT power supplies are quite expensive and bulky since they have to provide an electrical isolation of a few thousand volts through a high-voltage isolation transformer.

To reduce the cost and size of the power supplies for switching device gate drivers, three distinct designs without using isolation transformers were proposed in the literature. However, these designs were essentially for SCR and GTO devices, and cannot be adopted for GCTs. The main objective of this thesis is, therefore, to develop a novel low-cost self-powered supply for GCT devices, where the costly high-voltage isolation transformer is eliminated. To achieve this objective, the thesis will address and solve the following technical challenges and difficulties.

- 1) **Maximum energy transfer from snubber capacitor to the proposed SPS without affecting snubber circuit operation.** Depending on the GCT current rating, its power supply is normally in the range of 10W to 60W. The proposed SPS should be designed to obtain sufficient energy from the GCT snubber capacitor while the operation of the snubber circuit should not be affected.
- 2) **Regulated output voltage with an electrical isolation.** Most of GCT device requires a stable output voltage of 20V with a maximum error of $\pm 0.5\%$. Therefore, the output voltage of the SPS should be controlled with a good voltage regulation. Further, it is required that the proposed SPS provides a low-voltage isolation between its input and output.
- 3) **Low cost and compact size.** In addition to the elimination of high-voltage isolation transformer for cost reduction, the proposed SPS should not add any costly components with high voltage or high current to the power circuit. The component count of the SPS should be minimized as well.
- 4) **Simple and practical simulation model.** To assist the analysis and design of the proposed SPS, a simple and practical simulation model for GCT gate drivers and proposed SPS should be developed.

- 5) **Experimental verification.** To verify the simulation results and performance of the proposed GCT power supply, a prototyping GCT supply should be developed and tested.

1.3 Thesis Organization

This thesis consists of five chapters. The technical background, literature review, and existing power supply techniques for SCR and GTO gate drivers are presented in the first chapter. The main objectives of the thesis are discussed.

In Chapter 2, a novel self-powered supply for GCT gate drivers is proposed. The operating principle of the proposed SPS circuit is elaborated. Theoretical analysis is conducted and design guidance is provided.

Chapter 3 emphasizes the modeling and analysis of the proposed power supply. Simplified simulation models for GCT gate drivers are developed. The performance of the SPS is then investigated by simulation. The relationship between the SPS maximum output power and its parameters is identified. The SPS start-up process is also discussed.

Chapter 4 provides the experimental verification of the proposed SPS. A laboratory prototype is designed and built to verify the performance of the proposed power supply. A variety of experiments on the SPS are conducted. The experimental waveforms under different operating conditions are analyzed.

Chapter 5 provides the conclusions of the thesis. Other relevant supporting materials are attached in appendices.

CHAPTER 2

PRINCIPLE OF SELF-POWERED SUPPLY FOR GCT GATE DRIVERS

2.1 Introduction

As introduced in Chapter 1, self-powered supply (SPS) techniques for GTOs and SCRs are not suitable for GCTs since the gating requirements for GCTs are much different from these switching devices. A novel self-powered supply for the GCT gate driver is, therefore, proposed in this chapter. The supply obtains energy from the GCT snubber circuit and then converts the energy into a regulated 20V dc supply to drive the GCT gating circuits. Hence the expensive and bulky isolation transformers used in commercial power supplies for GCT gate drivers can be eliminated.

This chapter starts with an introduction to the novel self-powered supply for GCT gate drivers, followed by a detailed discussion on its operating principle. The design requirements for the proposed supply are provided. The charging technique and the principle of output voltage regulation are analyzed. The design methods for maximum output power and optimum start-up process are also presented.

2.2 Technical Requirements and Configuration of the Proposed SPS

Fig. 2-1 shows the simplified circuit diagram of a PWM current source rectifier used in high-power drives as a front end converter, where the proposed self-power supplies are employed

for GCT devices in the rectifier. The rectifier essentially consists of six symmetrical GCT switches, S_1 to S_6 , which are protected by six sets of RC snubber circuits, R_s and C_s . The proposed self-powered supplies (SPS) are in series with the snubber circuits. The principle of the self-powered supply is to utilize the energy stored in the snubber capacitor C_s to drive the GCT gating circuit. Since the snubber circuit is at the same potential as the GCT device, the insulation level of the self-powered supply is reduced from thousands of volts to a couple of hundreds volts [15,16].

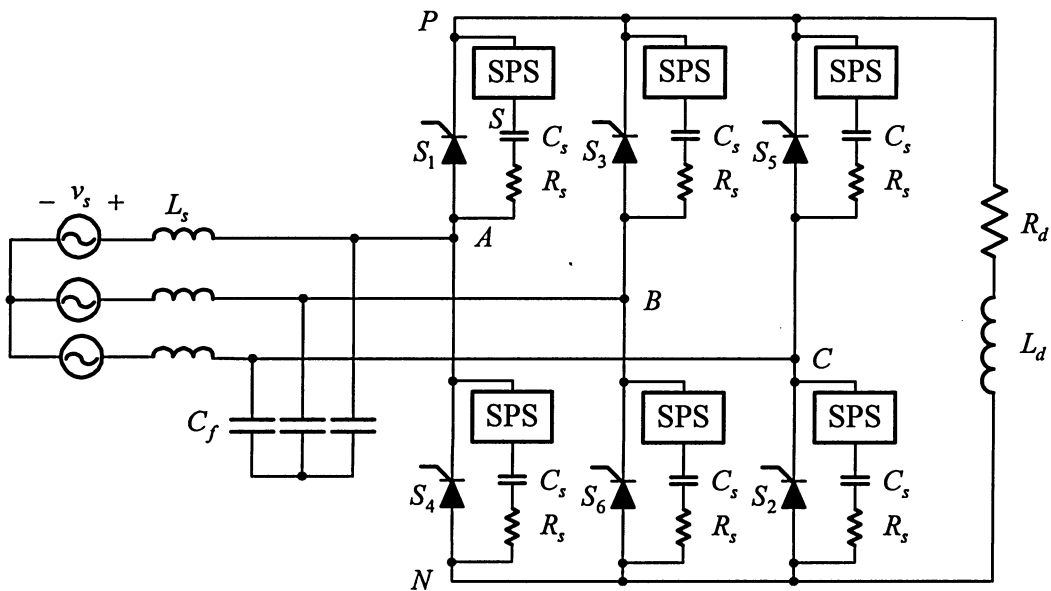


Fig. 2-1 PWM Current Source Rectifier (CSR) with six self-powered supplies.

2.2.1 Technical Requirements

As the GCT gating requirements are much different from those of other devices, the proposed SPS should meet following requirements:

1) Effective energy transfer to the GCT gate driver

The gating of GCTs requires much more energy, typically up to 60W, than that of GTOs or SCRs. A major portion of the required energy is transferred to the gate driver during the GCT turn-off [15]. Another portion of the energy is dissipated for turning on the GCT device including the generation of turn-on pulse and back-porch current. The third portion, around 5W, is the gate driver component dissipation. Obviously, the supply should be designed to fulfill the total power requirement for GCT gate drivers.

2) No effect on snubber circuit operation

Since the snubber circuit is used to protect the device during switching, its function should not be influenced under any circumstances. Therefore, the proposed SPS should not affect the operation of the snubber circuits [16].

3) Regulated output voltage

Since the load conditions during different switching periods of the gate driver are distinct, and the voltage requirement ($20 \pm 0.5V$) of the power supply for GCT gate driver is critical, the output voltage of the designed SPS must be regulated in order to achieve reliable GCT switching.

4) Voltage isolation between snubber circuit and the GCT gate driver

The GCT is switched on or off by a positive or negative current through the gate and cathode of the GCT. In order to ensure the power supply working properly, the isolation should be provided between the snubber circuit and the gate driver. The detailed operations and

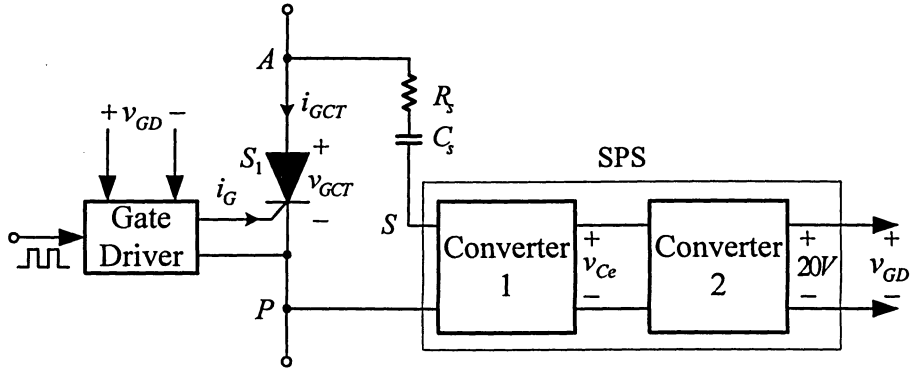
explanations are given in Appendix C.

Based on the above requirements, a novel self-powered supply is designed. The circuit configuration and analysis are given in following sections.

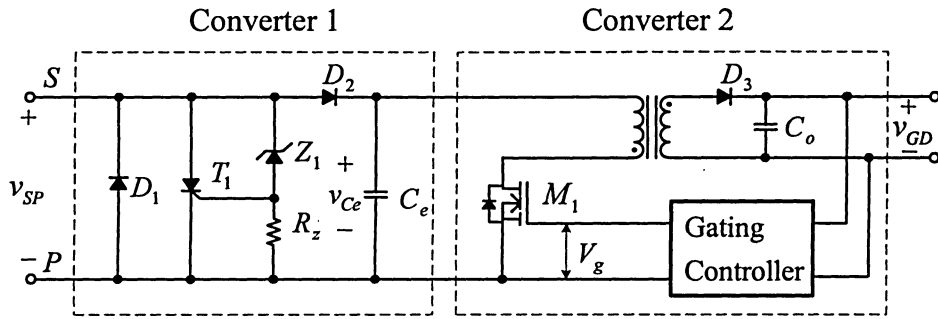
2.2.2 SPS Configuration

The block diagram of the proposed self-powered supply is shown in Fig. 2-2(a). The supply consists of two converters: Converter 1 and Converter 2. The main functions of Converter 1 are to transfer the energy from the snubber capacitor C_s to the energy-storage capacitor C_e and to minimize possible interference to the snubber circuit operation. Converter 2 converts the unregulated dc voltage v_{Ce} to a regulated dc voltage v_{GD} for the GCT gate driver, and also provides insulation between the snubber circuit and the gate driver.

Fig. 2-2(b) shows a circuit diagram of the proposed SPS. When a positive voltage is established between the terminals S and P, a current flows through diode D_2 to charge the energy storage capacitor C_e . Once v_{Ce} reaches its maximum value V_{max} , set by the zener diode Z_1 , the diode Z_1 will breakdown and conduct, causing thyristor T_1 to conduct. The current from S to P is thus diverted from C_e to T_1 . In this case, diode D_2 is reverse-biased, preventing C_e from discharging through T_1 . When the voltage between S and P becomes negative, the diode D_1 will conduct, providing a current path for the snubber circuit. Moreover, in order to minimize the impact of the SPS on the snubber operation, C_e should be much greater than C_s .



(a) Block diagram.



(b) Circuit diagram of SPS.

Fig. 2-2 Circuit diagram of the self-powered supply for GCT gate drivers.

Converter 2 is essentially a flyback converter, which converts the unregulated dc voltage on C_e to a regulated dc voltage v_{GD} for the gate driver. This converter consists of a power MOSFET, a high-frequency transformer and a controller. The transformer produces a step-down voltage and provides the required isolation (hundreds of volts) between the RC snubber circuit and the GCT gate driver. Based on the output feedback, the duty cycle of the MOSFET is controlled, so that the dc output voltage of the converter v_{GD} is regulated at $20V$.

2.2.3 Converter 1 for Energy Storage

Converter 1 is utilized to store energy transferred from the snubber circuit. The detailed operating principle of this converter and the self-powered technique are elaborated in this

section.

1) Typical waveforms

Fig. 2-3 illustrates typical waveforms during the charging process of the energy storage capacitor C_e in a medium voltage (MV) current source rectifier (CSR). The rectifier is rated at 2300V (line-to-line voltage) and 0.4MVA. Each GCT device in the rectifier is turned on for 120° and turned off for 240° per fundamental-frequency cycle. In Fig. 2-3, v_{GCT} is the GCT voltage, v_{Cs} is the snubber capacitor voltage, v_{Ce} is the voltage across the energy storage capacitor, and i_{GCT} is the GCT current waveform. It can be observed that when the GCT is turned on, v_{GCT} is equal to zero. However, when the GCT is turned off, the v_{GCT} can either be positive ($v_{GCT} > 0$) or negative ($v_{GCT} < 0$).

The snubber capacitor voltage v_{Cs} follows the GCT voltage v_{GCT} with a time delay caused by the RC snubber circuit. The voltage across the energy storage capacitor C_e is a function of GCT switching status. When the GCT is turned on, the capacitor C_e discharges its energy to the gate driver through Converter 2, causing decrease of v_{Ce} . While the GCT is turned off, the capacitor C_e will be charged. In Fig. 2-3, it can be observed that the capacitor C_e , as long as $dv_{GCT}/dt > 0$, can be charged under both conditions of $v_{GCT} > 0$ and $v_{GCT} < 0$. Each condition has different current paths and is discussed in detail in following sections.

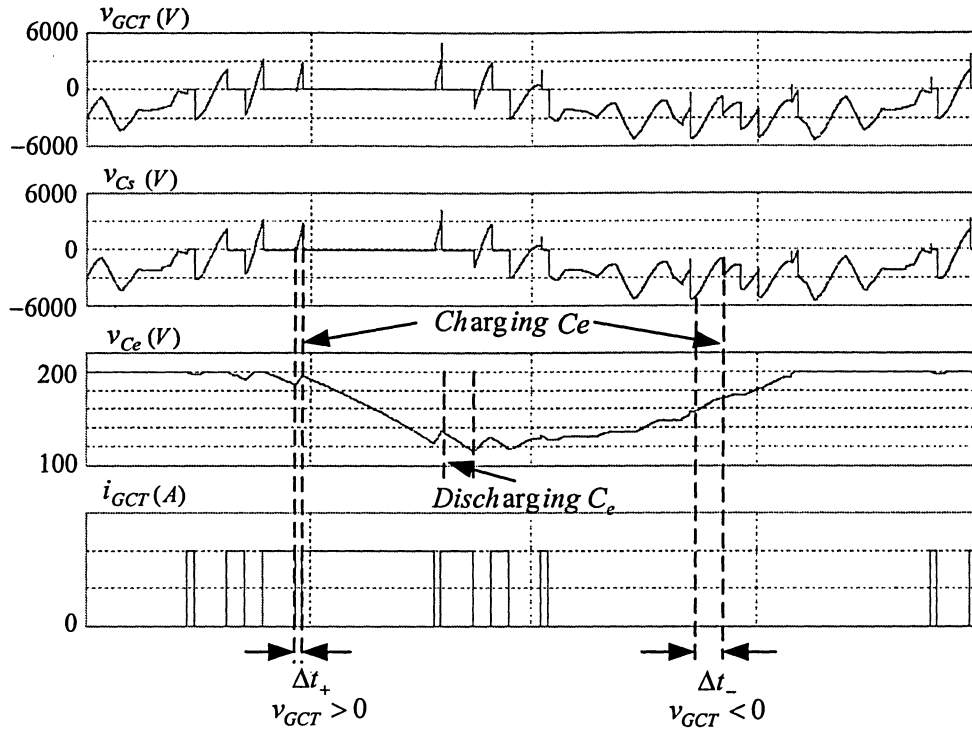
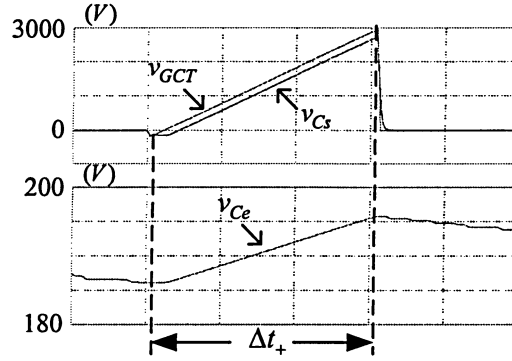


Fig. 2-3 Typical voltage and current waveforms for GCT device and capacitors.

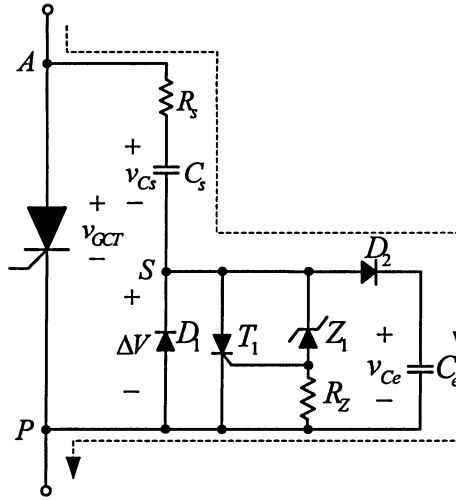
2) Charging of C_e with $v_{GCT} > 0$

Fig. 2-4(a) shows the voltage waveforms of charging the storage capacitor C_e with $v_{GCT} > 0$. Assume that the GCT switch is initially turned on and the voltage on the snubber capacitor is zero. When the switch is turned off during Δt_+ , its voltage v_{GCT} starts to increase and the GCT current begins to divert to the snubber circuit and the SPS. Consequently, the voltage across the energy storage capacitor v_{Ce} increases, and the electric energy is transferred into the Converter 1. The current path during the charging process is shown in Fig. 2-4(b) with dashed line. Once v_{Ce} reaches its maximum value V_{max} set by Z_1 , the thyristor T_1 will be fired. The snubber current will be diverted from C_e to T_1 . As a result, diode D_2 will be reverse-biased,

preventing C_e from discharging through T_1 .



(a) Waveforms.



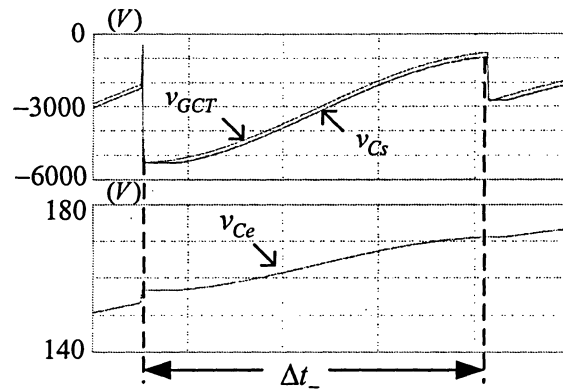
(b) Current paths

Fig.2-4 Charging process with $v_{GCT} > 0$.

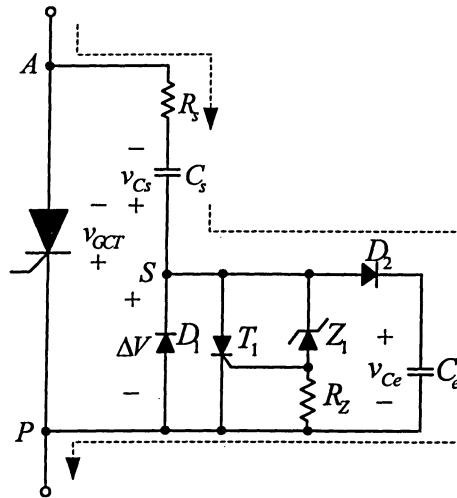
3) Charging of C_e with $v_{GCT} < 0$

The energy storage capacitor C_e can also be charged when $v_{GCT} < 0$. The charging process is shown in Fig. 2-5. During Δt_- , v_{GCT} increases from $-6200V$ to $-1000V$ due to the

operation of other GCTs in the rectifier. The snubber capacitor voltage v_{Cs} has an initial voltage of $-6200V$ and will follow the increment of v_{GCT} with a short delay, which is caused by the RC circuit. Obviously, $|v_{Cs}|$ is greater than $|v_{GCT}|$ in this situation. Thus the input voltage ΔV of the SPS circuit, given by $\Delta V = v_{GCT} - v_{Cs}$, is always positive. Once ΔV becomes greater than v_{Ce} , the snubber capacitor C_s starts to discharge and release its stored energy to C_e .



(a) Waveforms



b) Current paths

Fig. 2-5 Charging process for $v_{GCT} < 0$.

In summary, the energy storage capacitor C_e can be charged when $v_{GCT} > 0$ and $v_{GCT} < 0$. This greatly improves the energy transfer capability of proposed self-powered supply.

2.2.4 Converter 2 for Regulated DC Output Voltage

1) Circuit diagram

Fig. 2-6 shows the circuit diagram of Converter 2. It is essentially a flyback converter, which converts the unregulated dc voltage v_{Ce} to the regulated dc voltage v_{GD} to power the GCT gate driver. The converter consists of a power MOSFET M_1 , a high-frequency step-down transformer and a gating controller. The transformer provides not only a step-down voltage to the load but also an electric isolation between the RC snubber circuit and the GCT gate driver. Based on the sensed voltage feedback, the gating controller generates proper duty cycles of the gating signal for the MOSFET to keep v_{GD} at 20V. The fast closed-loop control and high switching frequency (132kHz) make v_{GD} fulfill the power supply requirement of the GCT gate driver.

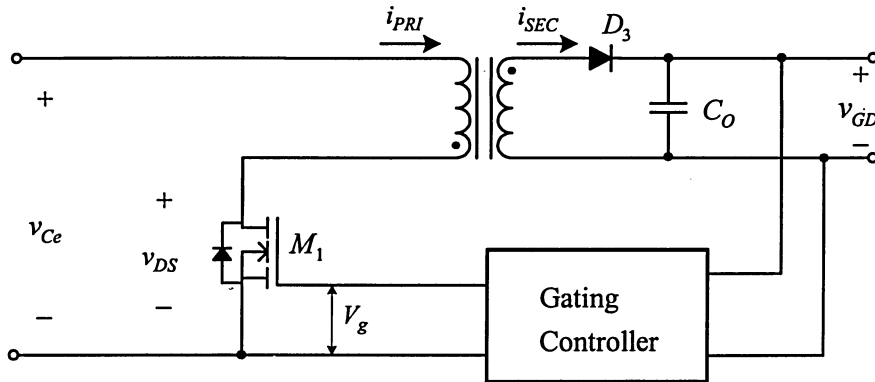


Fig. 2-6 Circuit diagram of Converter 2.

2) Operating modes

There are two different operating modes of flyback converters, discontinuous mode and continuous mode. Generally speaking, the converter will operate in a discontinuous current mode under light load conditions, and will move into the continuous mode when the output load current is increased beyond a unique boundary [17]. Both operating modes are analyzed in detail in this section.

a) Discontinuous mode

Fig. 2-7 shows typical waveforms of the flyback converter operating in a discontinuous mode, where each operating cycle contains three distinct intervals [18].

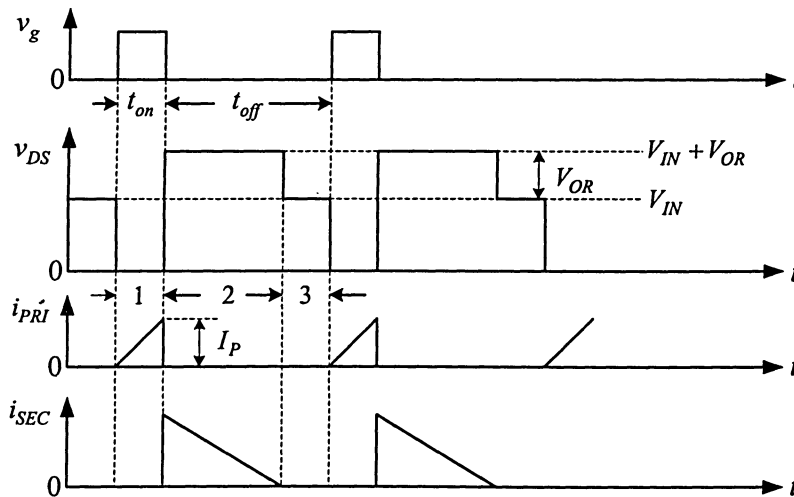


Fig. 2-7 Waveforms of the flyback converter operating in a discontinuous mode.

Interval 1 is the period that MOSFET is turned on. The transformer primary current i_{PRI} increases linearly over time because of the inductance of the flyback transformer. The MOSFET drain to source voltage $v_{DS(on)}$ is close to zero. The secondary current i_{SEC} is zero since the

output diode D_3 is reverse-biased, preventing current from flowing back. During this interval, energy is stored in the magnetic field of the transformer.

Interval 2 starts from turning off of the MOSFET, and ends with the exhausting of the secondary current i_{SEC} . Once the MOSFET is switched off, the voltages across both the primary and secondary windings are reversely polarized. Since the primary current i_{PRI} falls to zero by the MOSFET turn-on, the secondary current i_{SEC} instantly starts to charge the output capacitor C_o . The voltage across the secondary winding is equal to the sum of the output voltage and diode forward voltage. This voltage is referred to the primary side according to the turns ratio of the transformer. Thus the MOSFET voltage stress here is the sum of the reflected output voltage V_{OR} and the input voltage V_{IN} . During this interval, the magnetic energy stored in the transformer during the first interval is released to charge the output capacitor C_o and to power the load circuit.

Interval 3 begins at the moment when the secondary current i_{SEC} decays to zero, and ends with the beginning of the next cycle. The MOSFET drain to source voltage is equal to the input voltage of the converter. Both the primary and the secondary current are zero during this interval. That is the reason why this operating mode is defined as the discontinuous mode. As a result, the output load current is supplied by output capacitor C_o .

During each cycle of this mode, the energy delivered to the load by the transformer is:

$$E = \frac{1}{2} L_p I_p^2 \eta \quad (2-1)$$

where L_p is the transformer primary inductance in Henries, I_p is the peak value of i_{PRI} , and η is the transformer efficiency.

Thus the output power is defined by

$$P_o = \frac{1}{2} L_p I_p^2 \eta f_s \quad (2-2)$$

where f_s is the switching frequency of the MOSFET.

Furthermore, when the MOSFET is on, and the primary current in amperes is given by

$$i_{PRI} = I_I + \frac{(V_{IN} - V_{DS(ON)})t_{on}}{L_p} \quad (2-3)$$

where I_I is the initial value of the primary current, and t_{on} is the turn-on time of the MOSFET.

Substituting I_p in Equation (2-2) for I_{PRI} in Equation (2-3) with $I_I = 0$ and $V_{DS(ON)} = 0$, the output power of the flyback converter can be expressed as

$$P_o = \frac{V_{IN}^2 D^2 \eta}{2 L_p f_s} \quad (2-4)$$

where D is duty cycle defined by $D = \frac{t_{on}}{T_s}$, and T_s is the switching time period.

b) Continuous Mode

Fig 2-8 shows the waveforms of continuous mode operation for the flyback converter. The secondary current i_{SEC} of the continuous mode does not fall to zero during the MOSFET off period. There are only two intervals in the continuous mode. Interval 3 of the discontinuous mode does not exist here.

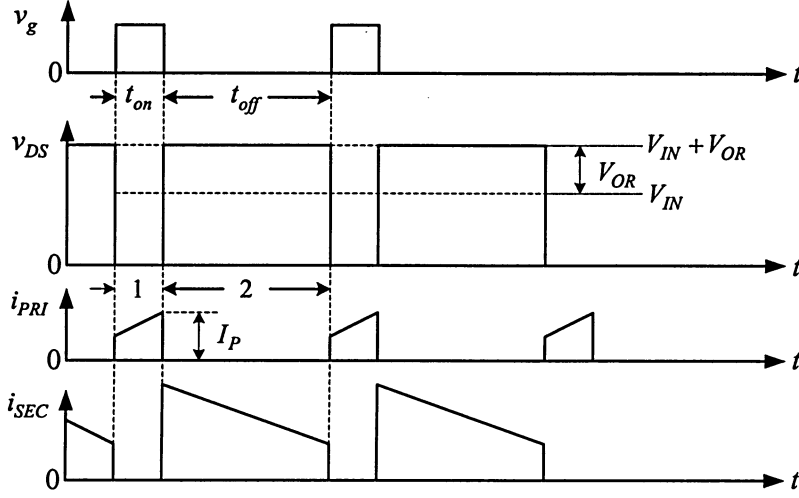


Fig. 2-8 Flyback converter waveforms – continuous mode.

When the MOSFET is turned on during Interval 1, the primary current i_{PRI} increases. Since the secondary current is continuous, the MOSFET voltage stress V_{DS} is different from that of the discontinuous mode.

In order to maintain a constant output voltage, the amount of current increase in the primary inductance during the MOSFET turn-on period must be balanced by the amount of current decrease during the MOSFET turn-off period. The above phenomenon leads to

$$\frac{(V_{IN} - V_{DS(ON)})D}{L_P f_S} = \frac{(V_{GD} + V_{D3})(1-D)}{\frac{N_s}{N_p} L_P f_S} \quad (2-5)$$

from which the output voltage v_{GD} of the converter can be expressed by

$$v_{GD} = \left[(V_{IN} - V_{DS(ON)}) \frac{D}{1-D} \frac{N_s}{N_p} \right] - V_{D3} \quad (2-6)$$

where N_p and N_s are number of turns of the primary and secondary windings, respectively.

The boundary current between the continuous and discontinuous modes is defined by

$$I_{OB} = \frac{V_{IN}^2 V_{GD}}{2 f_s L_p \left[\left(\frac{N_s}{N_p} V_{IN} \right) + V_{GD} \right]^2} \quad (2-7)$$

If the output current is greater than the boundary current I_{OB} , the converter operates with the continuous mode. Once the load current is lower than I_{OB} , the converter is in the discontinuous mode. The MOSFET switching frequency and the transformer primary inductance are inversely proportional to the I_{OB} while the input voltage V_{in} is directly proportional to I_{OB} .

In summary, the flyback converter converts the unregulated dc voltage on energy capacitor C_e to a regulated dc voltage v_{GD} , and provides the required isolation between the snubber circuit and the GCT gate driver.

2.2.5 Design Guidance for C_e and SPS Start-up Process

1) Design guidance for C_e

The value of energy storage capacitor C_e is determined by the amount of energy required for powering the GCT gate driver. In order to minimize the effect of SPS circuit on the RC snubber performance, C_e should be much greater than C_s . The energy stored in C_e can be expressed as

$$E = \frac{1}{2} C_e V_{Ce}^2 \quad (2-8)$$

In order to increase the energy stored in C_e , either C_e or V_{Ce} could be increased. Neglecting a small voltage drop across the snubber resistor and assuming $C_e \gg C_s$, the

voltage across the C_e can be calculated by

$$V_{Ce} = \frac{C_s}{C_e} V_{GCT} \quad (2-9)$$

This equation indicates that for a given GCT voltage V_{GCT} , an increase of C_e will cause a reduction of V_{Ce} . Therefore, the value of C_e and V_{Ce} should be appropriately selected to transfer sufficient energy from the snubber circuit to C_e . Since the stored energy is proportional to the V_{Ce} square, it is preferable to increase V_{Ce} rather than to decrease C_e for achieving maximum energy transfer.

2) SPS start-up process

The controller of Converter 2 has two special voltage settings, starting voltage V_{start} and minimum voltage V_{min} . They form a voltage hysteresis band as shown in Fig. 2-9. When the input voltage v_{Ce} of the flyback converter increases from zero, the MOSFET gate signal is prohibited and the MOSFET is disabled until $v_{Ce} > V_{start}$. Once the MOSFET is enabled, the variations of v_{Ce} cannot disable the operating of the MOSFET unless v_{Ce} falls lower than V_{min} . In general, V_{start} is preset to a value close to V_{max} to achieve more energy transfer during the start-up process. And V_{min} is usually set around 40% of V_{start} to optimize converter's operating performance.

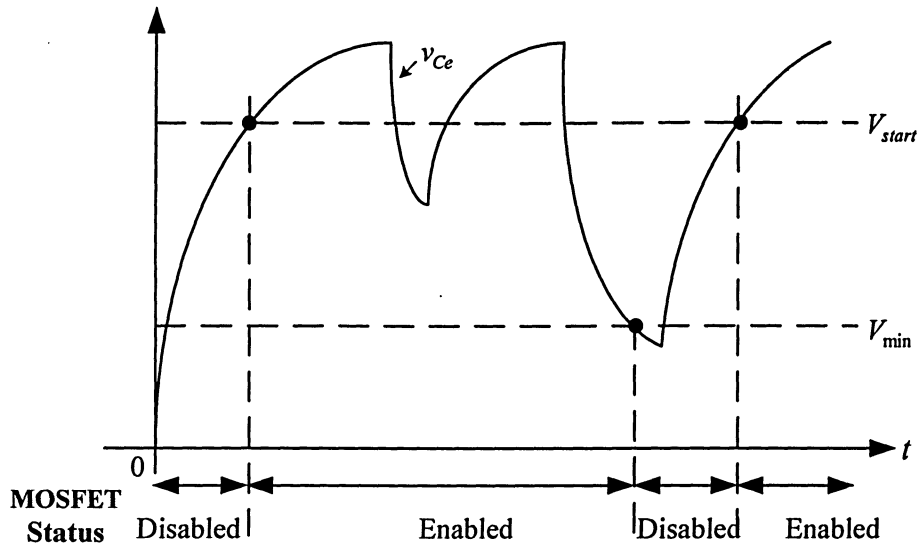


Fig. 2-9 V_{start} , V_{min} , v_{CE} and MOSFET operation status.

In summary, by selecting a proper value of the energy storage capacitor C_e and voltage level for this capacitor, the proposed SPS can transfer sufficient energy from the GCT snubber circuit. A proper design of the hysteresis voltage band in Converter 2 can provide a proper start-up process of the SPS.

2.3 Conclusion

In this chapter, a novel self-powered supply (SPS) for GCT gate drivers is proposed. The supply is composed of two power converters, Converter 1 and Converter 2. The former is used to transfer sufficient energy from the GCT snubber circuit to the SPS, whereas the later is utilized to regulate the output voltage of the supply and to provide electrical isolation between the SPS and its gate driver. The SPS design requirements are provided, and its operating principle is elaborated. Methods for efficient energy transfer from the GCT snubber circuit to the SPS are discussed and the SPS start-up process is introduced.

24

CHAPTER 3

MODELING, SIMULATION AND ANALYSIS

3.1 Introduction

This chapter deals with modeling, simulation, and analysis of the proposed self-powered supply (SPS) for GCT gate drivers. The GCT gate driver is a complex circuit to produce specially defined gate current waveforms for the turn-on and turn-off of a GCT thyristor [19]. The gate driver contains many digital and analog components, which are difficult to model by computer software such as PSIM. To facilitate computer simulation and analysis of the proposed self-powered supply, a simple and effective model for the GCT gate driver should be developed. With a suitable model in place, the performance of the SPS can be analyzed and its maximum output power can be investigated.

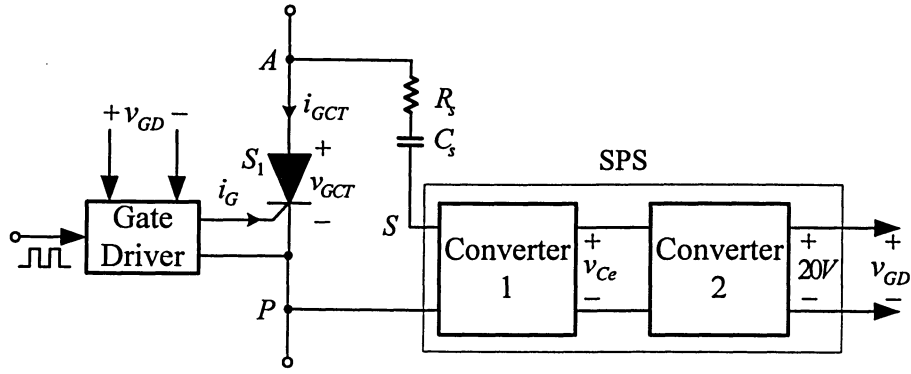
This chapter starts with the development of a simplified simulation model for the GCT gate driver, followed by modeling of the proposed SPS using commercial software PSIM. These two models are then integrated for the investigation of SPS maximum output power. The relationship between the SPS output power and system parameters is examined, and the SPS startup process is analyzed.

3.2 Modeling of SPS and GCT Gate Driver

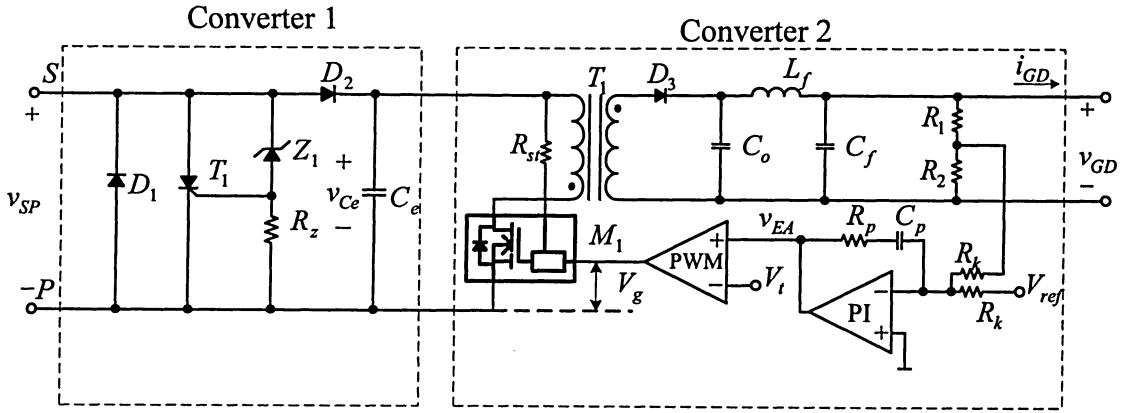
3.2.1 Modeling of Self-Powered Supply (SPS)

Fig. 3-1 shows the block diagram and detailed schematics of the self-powered supply for

GCT gate driver, respectively. As introduced in Chapter 2, the SPS consists of two converters, Converter 1 and Converter 2. The function of Converter 1 is to transfer sufficient energy from the snubber circuit to the energy storage capacitor C_e . Converter 2 is a flyback dc-dc converter, which converts the unregulated dc voltage on C_e to a regulated dc voltage v_{GD} for the GCT gate driver. This converter includes a high-frequency step-down transformer T_1 , which provides isolation between the SPS and the GCT gate driver and hence isolates the supplied voltage v_{GD} from the snubber circuit. Diode D_3 and capacitor C_o are the output rectifier and output capacitor of Converter 2, respectively. The inductor L_f and the capacitor C_f form a low pass filter to attenuate ripples of the output voltage. A MOSFET M_1 is controlled by a regulator circuit, which contains a PI compensator and a PWM generator. The SPS output voltage v_{GD} is detected by R_1 and R_2 , and is then compared with a reference voltage V_{ref} . The error is processed by the PI controller. The output of the PI controller v_{EA} is compared with a periodic sawtooth voltage V_t in the PWM generator, which produces pulse width modulated rectangular waveforms to drive M_1 . Moreover, the resistor R_{sr} is used to set the input start-up voltage V_{start} and the minimum voltage V_{min} of Converter 2. The definitions of V_{start} and V_{min} are provided in Chapter 2 and illustrated in Fig. 2-9.



(a) Block diagram.



(b) Circuit diagram.

Fig. 3-1 Circuit diagram of the SPS for the GCT gate driver.

3.2.2 Modeling of GCT Gate Driver

The GCT device is essentially a GTO thyristor integrated with a special gate driver with an extremely low gate inductance (typically $< 5\text{nH}$) [1]. For a 4.5kV/4kA GCT, the total inductance in the gate driver loop is about 3nH such that a di_{GQ}/dt (the critical rate of rise of turn-off gate current) of greater than $6000\text{A}/\mu\text{s}$ can be achieved. The gate driver with very low inductance, high di/dt improves the turn-on capability of the GCT as well [20,21].

Using a 4.5kV/4kA GCT device, an anode current of 4000A can be turned off with the turn-off storage time of $3.0\mu\text{s}$ and di_{GQ}/dt of $6000\text{A}/\mu\text{s}$. Table 3.1 gives the specifications

of the 4.5kV/4kA GCT device and its gate driver [22].

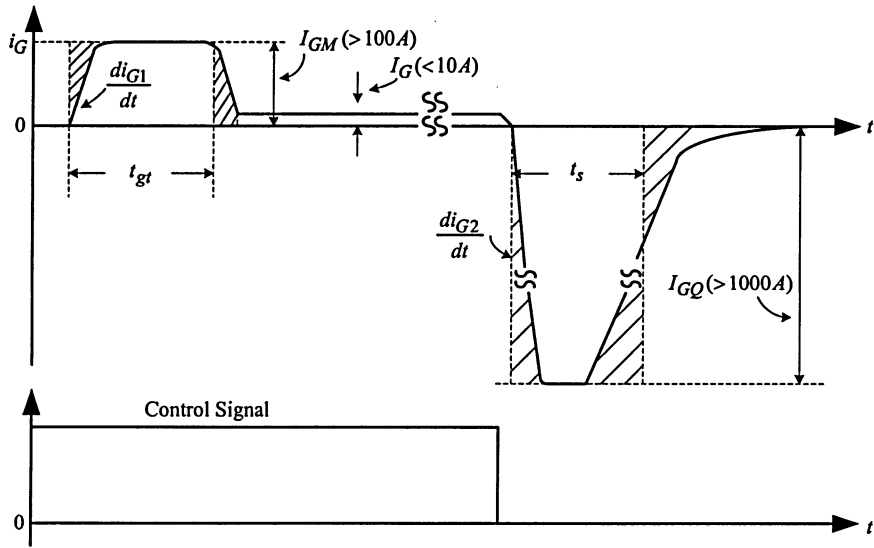
Table 3.1 Specifications of 4.5kV/4kA GCT.

| GCT Device (FGC4000BX-90DS) | | |
|---|----------------|-----------------|
| Repetitive peak off-state voltage | V_{DRM} | 4500A |
| Repetitive controllable on-state current | I_{TORM} | 4000A |
| Storage time | t_s | 3.0 μ s |
| Turn on time | t_{gt} | 3.0 μ s |
| Gate Driver (GU-C40) | | |
| Power supply voltage | V_{GD} | 21V |
| Peak on gate current | I_{GM} | 200A |
| Peak off gate current | I_{GQ} | 4000A |
| Critical rate of rise of on gate current | di_G / dt | 100A / μ s |
| Critical rate of rise of off gate current | di_{GQ} / dt | 6000A / μ s |

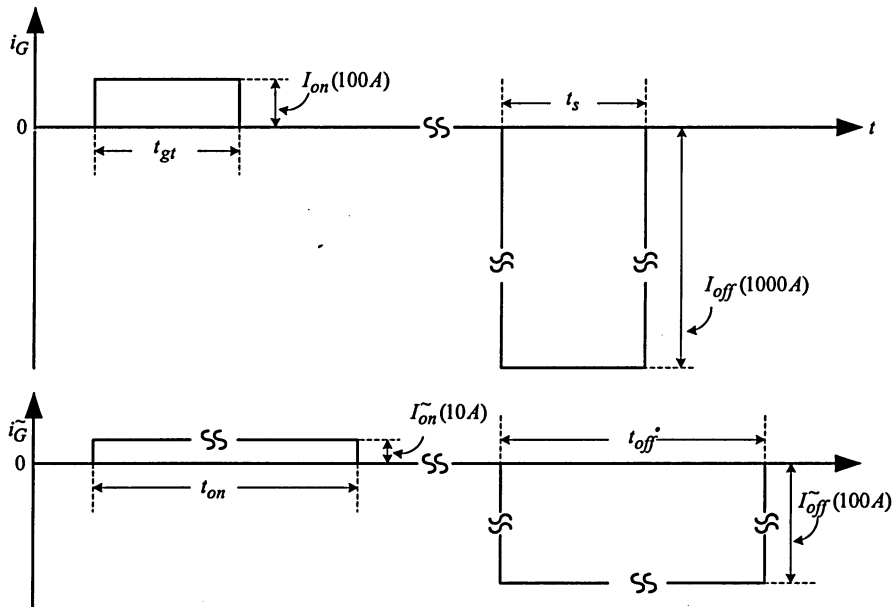
Fig. 3-2(a) shows the typical waveform of the gate current i_G for a GCT device [1, 22]. When the turn-on signal is applied, the gate current starts to increase after a short time delay. The rate of rise of the gate current di_G / dt should be greater than 100A / μ s, and its peak value I_{GM} should be more than 100A. After the GCT device is fully turned on, it only requires a

back-porch current of lower than $10A$ to keep the device conducting. The power dissipated in this period is much lower than that in the turn-on or turn-off period. Once the turn-off signal is generated, a negative turn-off gate current will be produced after a short time delay. The peak value of the gate current I_{GQ} can be greater than $1000A$, and the di_{GQ}/dt can be higher than $6000A/\mu s$. Such a great I_{GQ} and high di_{GQ}/dt can substantially reduce the turn-off time of the GCT. During this period, much more energy is dissipated in comparison with the case in the turn-on period [23, 24].

To simplify the analysis, the actual GCT gating current waveforms can be replaced by those given in Fig. 3-2(b), where the gate currents at turn-on and turn-off are replaced by two dc currents I_{on} and I_{off} . The back-porch current is neglected due to its lower power dissipation. The corresponding switching times for I_{on} and I_{off} are the turn-on time t_{gt} and turn-off time t_s , respectively. Since t_{gt} and t_s are typically $3\mu s$, a very small simulation time step, such as $0.1\mu s$, must be used for accurate simulation of the SPS. As a result, the simulation time will be unnecessarily long. To maintain simulation accuracy and shorten simulation time, t_{gt} and t_s are prolonged to t_{on} and t_{off} , while the magnitudes of the turn-on gate current I_{on} and turn-off gate I_{off} are proportionally reduced to \tilde{I}_{on} and \tilde{I}_{off} , respectively.



(a) Typical waveform



(b) Proposed waveform

Fig. 3-2 GCT turn-on and turn-off gate current waveform.

Fig. 3-11 t_2 versus C_e .

3.5 Summary

In this chapter, a simulation model for the proposed self-powered supply (SPS) is developed. In order to simulate the GCT gate driver efficiently, a simplified model for the gate driver is proposed, based on which the performance of the SPS is investigated. The relationship between the SPS maximum output power $P_{O,\max}$ and its parameters, including energy storage capacitance C_e and its maximum voltage V_{\max} , snubber capacitor C_s , and utility supply voltage V_{LL} , is analyzed. The proposed SPS can provide an output power of more than $60W$, which can meet the requirement of most commercial GCT devices. The startup process of the SPS for PWM current source rectifiers is also investigated.

CHAPTER 4

EXPERIMENTS

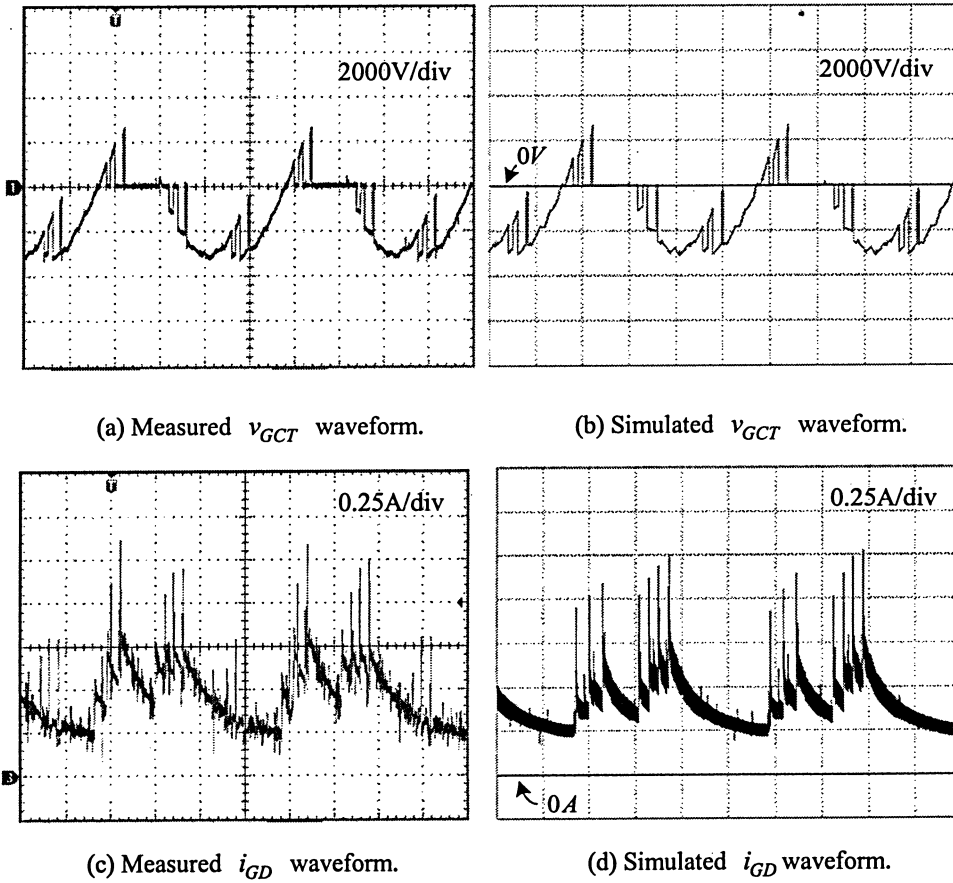
This chapter addresses two major experimental tasks. One task is to verify the proposed simulation model for GCT gate drivers. As indicated in the previous chapter, the GCT gate driver is a complex circuit, and a suitable model for the gate driver can facilitate the simulation of the proposed self-powered supply (SPS). The experiments for this task are conducted on a 4160V 400KW current source drive. The second experimental task is to verify the performance of the self-powered supply. A prototype SPS of 60W is designed and built. Various experiments are carried out for the SPS operating under different conditions.

4.1 Verification of Simulation Model

To verify the gate driver model developed in Chapter 3, tests were carried out on a medium voltage drive at Rockwell Automation Canada. The drive system consists of a current source rectifier (CSR) and a current source inverter (CSI) with two symmetrical GCT devices in series in each switch position. The selective harmonic elimination (SHE) modulation scheme is used to eliminate the low-order harmonics. The operating conditions of the drive system are given in Table 4-1.

Table 4-1 Operating parameters of the tested drive system.

| Rated Line Voltage | Rated Output Power | DC Current | Motor Speed | Harmonic Elimination | Switching Frequency | Rectifier Firing Angle |
|--------------------|--------------------|------------|-------------|--|---------------------|------------------------|
| 4160V | 400KW | 79A | 1200RPM | 5 th , 7 th , and 11 th | 420HZ | 27.6° |



Timebase: 4ms/div

Fig. 4-1 Experimental waveforms for v_{GCT} and i_{GD} .

Fig. 4-1 shows the measured and simulated waveforms of v_{GCT} and i_{GD} , where v_{GCT} is the voltage across a GCT device and i_{GD} is the output current of a commercial GCT gate driver

power supply. When the GCT is turned on, v_{GCT} is equal to zero, while with the turn-off of the GCT, v_{GCT} can be either positive ($v_{GCT} > 0$) or negative ($v_{GCT} < 0$). The supply current i_{GD} contains narrow current spikes, caused by the switching of the GCT device. It can be observed that the measured waveforms match the simulated waveforms very well.

4.2 SPS Prototype

Figure 4-2 shows the picture of the laboratory prototype developed to verify the performance of the proposed SPS. The prototype is built based on the circuit shown in Figure 2-2. As shown in this figure, a 6.5kV/1.5kA GCT device with its gate driver is supplied by the SPS prototype. The gate signal from a DSP board will control the switching of the GCT device. To reduce the gate inductance and store a large amount of energy to turn on/off the GCT, numerous dc capacitors are mounted on the gate driver board. Depending on the size of GCTs, the value of the total capacitance is typically from $20,000\mu F$ to $50,000\mu F$ as discussed in the previous chapters.

The input terminal the prototype of the proposed SPS is connected with a snubber circuit to transfer energy to power the GCT gate driver. Two parallel capacitors standing on the left side of the board are the energy storage capacitors. A MOSFET integrated with a controller (Topswitch-GX) is mounted below the energy storage capacitors. A small high-frequency step-down transformer is installed above the MOSFET. Three output capacitors and an L-C filter are placed on the right side of the transformer. On the right side of the MOSFET are components of the output feed back circuit. The output terminal is on the right side of the board for connection to the GCT gate driver. The detailed schematics of the SPS board are given in Appendix D.

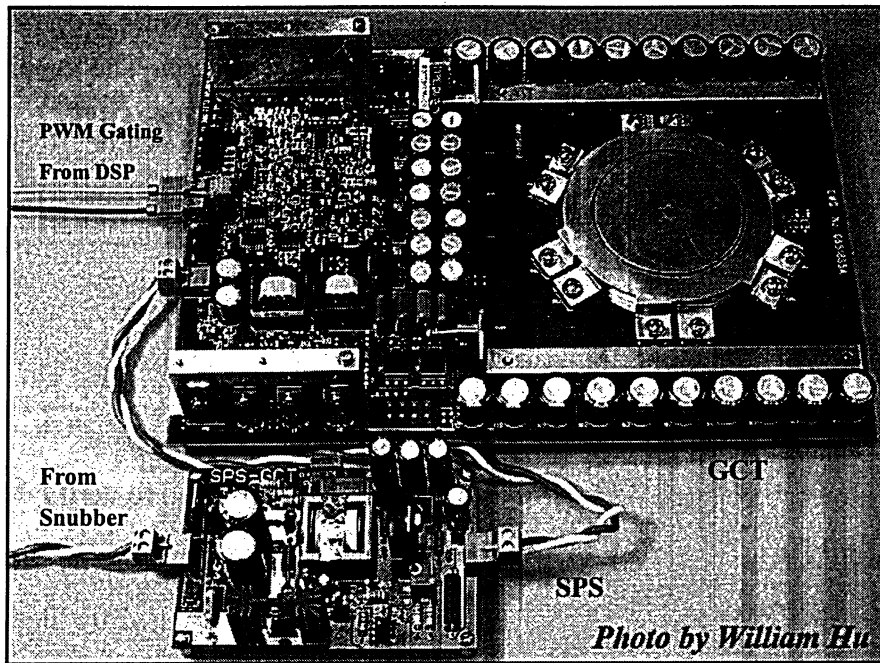


Fig. 4-2 GCT gate driver and SPS Prototype.

4.3 Experiments on SPS

The SPS prototype shown in Fig. 4-2 was tested to verify the performance of the proposed SPS technology. Since the medium voltage GCT converters were not available in Ryerson's Laboratory for Electric Drive Applications and Research (LEDAR), the experiments were conducted using a dc voltage, v_{in} , to emulate the voltage from the GCT snubber circuit. The simplified circuit diagram for the prototype is shown in Fig. 4-3, and the parameters of the SPS board are listed in Table 4-2. The schematic of the PCB board is given in Appendix D.

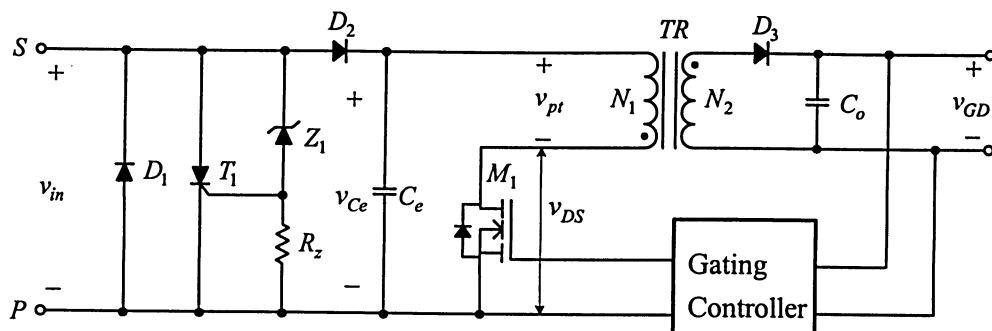


Fig. 4-3 Simplified SPS circuit diagram.

Table 4-2 Parameters of the SPS prototype

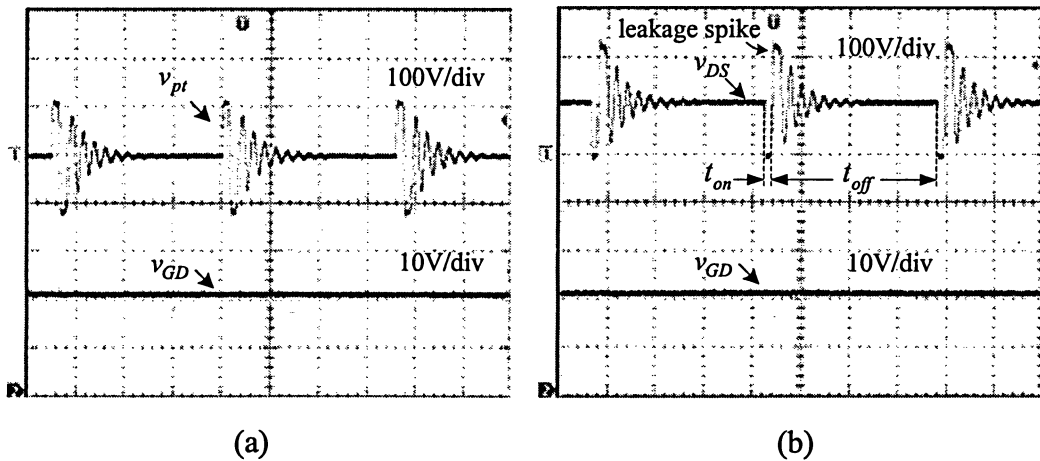
| Name | Definition |
|-------|--|
| D_1 | MUR6040, 400V/60A |
| T_1 | MCR106-6, 600V/4A |
| Z_1 | 2EZ200D5, 200V/2W |
| R_z | 100Ω/3W |
| D_2 | MUR460RL, 600V/35A |
| C_e | 66μF/450V |
| M_1 | Topswitch250, 700V/6.7A |
| TR | LSPA10703, rated voltage 3000V, $N_1/N_2 = 44/8$ |
| D_3 | MBR200100, 100V/20A |
| C_o | 2000μF/35V |

4.3.1 Constant dc Input Voltage

To verify the performance of the proposed SPS, experiments are conducted on the SPS prototype. For the tests discussed in this section, the SPS input voltage, v_{in} , is set at 100V and the SPS output power varies from zero to 60W, which covers the continuous and discontinuous current modes of operation.

1) No load condition

The SPS can satisfactorily operate under no load condition since the MOSFET M_1 has a Light Load Frequency Reduction function. This feature allows a power supply operating at lower switching frequencies under light load conditions to decrease the switching losses while maintaining good voltage regulation and low output ripple. Therefore, the SPS does not need any dummy loads [25].



Timebase: 4 μs/div
Fig. 4-4 Waveforms of the SPS on no load condition

Fig. 4-4 (a) shows the waveforms of v_{gs} and v_{ds} when the SPS is operating without any

load. Under this condition, only a small part of energy is delivered to the second side of the transformer, which is dissipated by components on the SPS board. Thus the turn-on time of the MOSFET, t_{on} , is very short as shown in Fig. 4-4 (b), during which the voltage across its drain and source v_{DS} is zero.

When the MOSFET is turned off, the energy stored in the transformer during the turn-on period is now transferred to the secondary circuit. However, the primary and secondary leakage inductances (L_{kp} and L_{ks}) are trying to oppose the change of their corresponding currents. Therefore, a “crossover region” occurs, during which the primary current ramps down and the secondary current ramps up. This transition excites the resonant tank circuit formed by the primary self-inductance of the transformer and the stray capacitance of the supply to create a decaying oscillatory waveform [25, 26].

2) 40W output power (discontinuous current mode of operation)

Fig. 4-5 shows the measured voltage waveforms of the SPS operating in a discontinuous mode, where the output power is 40W and the output voltage v_{GD} is kept constant at 20V. As shown in Fig. 4-5 (b), the discontinuous mode operation can be divided into three intervals per switching cycle. During Interval 1, the turn-on time of the MOSFET is significantly increased compared with that under no load conditions since more energy is delivered to the secondary side of the transformer. During Interval 2, the MOSFET is turned off, the oscillations at the moment when the MOSFET is turned off is caused by the LC resonant circuit formed by primary leakage inductance L_{kp} and the stray capacitance.

During Interval 3, the transformer magnetic field releases all its stored energy to the load.

This transition excites another LC resonant circuit formed by the primary self-inductance L_p and the stray capacitance, during which the oscillations persist until the MOSFET turns on again. Since the primary self-inductance L_p is much higher than the leakage inductance L_{kp} , the oscillation frequency is greatly reduced.

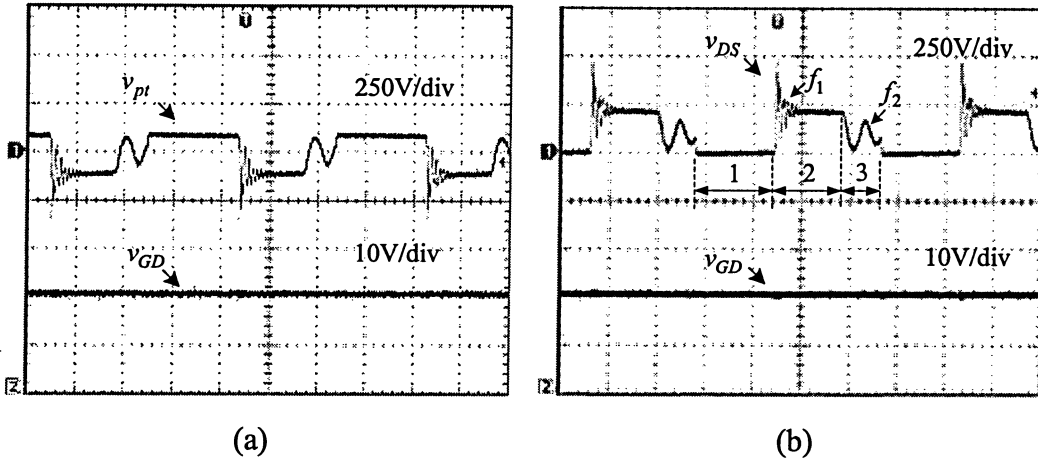


Fig. 4-5 Waveforms of the SPS operating in a discontinuous mode.

3) 60W output power (continuous mode)

When the output load current is increased, the SPS will operate in a continuous mode. Fig. 4-6 shows the voltage waveforms of the SPS in the continuous mode with a 60W output power. As illustrated in the figure, the switching cycle of the continuous mode contains two operation intervals. The operation of SPS during Intervals 1 and 2 are similar to those under the discontinuous operation. However, interval 3 in the discontinuous mode does not exist here. The SPS output voltage is regulated at 20V.

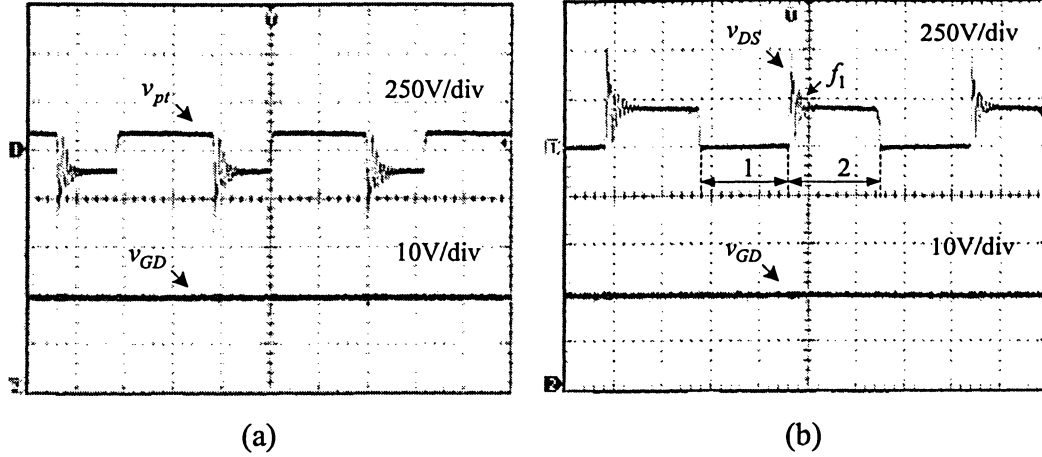
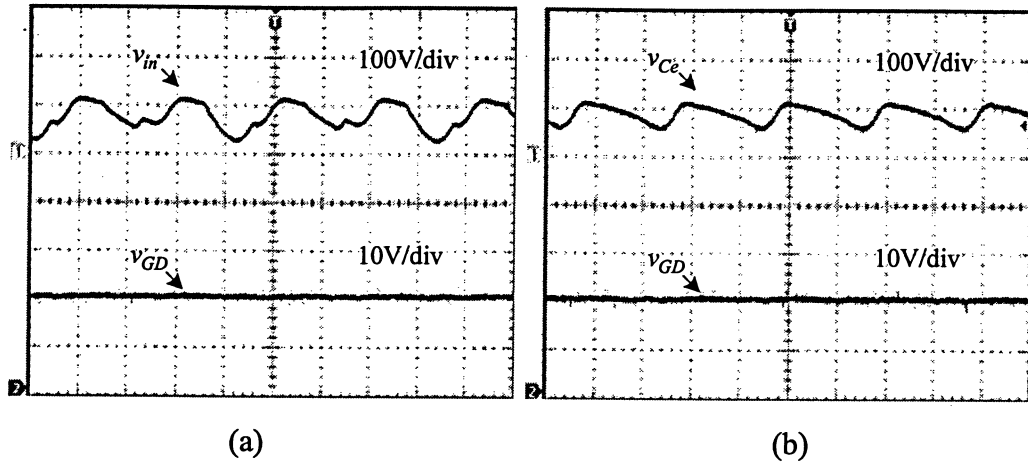


Fig. 4-6 Waveforms of the SPS operating in a continuous.

4.3.2 Input Voltage with High Fluctuation

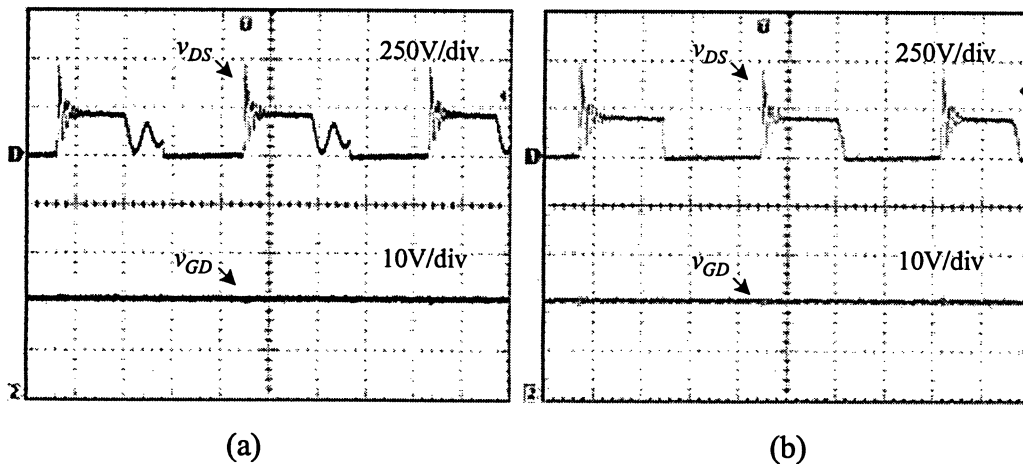
To further verify the performance of the prototype, the SPS is supplied by a highly fluctuated dc input voltage. Fig. 4-7 shows the waveforms of the SPS input voltage v_{in} , energy storage capacitor voltage v_{C_e} , and SPS output voltage v_{GD} . Because of the filtering of the energy storage capacitor C_e , v_{C_e} shown in Fig. 4-7(b) is smoother than v_{in} in Fig. 4-7(a). It is evident from the waveforms that the SPS can provide a stable output voltage v_{GD} despite the large fluctuations of the input voltage v_{in} .



Timebase: 4ms/div

Fig. 4-7 Highly fluctuated input voltage and stable SPS output voltage.

The waveforms of the SPS operating at 40W discontinuous and 60W continuous modes with a highly fluctuated input voltage are illustrated in Fig. 4-8 (a) and (b), respectively. Because of the superior performance of the flyback converter, the SPS dc output voltage can be kept constant.



Timebase: 2μs/div

Fig. 4-8 Discontinuous and Continuous modes waveforms of the SPS with a fluctuated input voltage.

4.3.3 Verification of Hysteresis Band of the MOSFET Controller

To verify the performance of the hysteresis band of the MOSFET controller, the SPS board is supplied by a power waveform generator which can generate step-up and step-down voltages. Fig. 4-9 shows the waveforms of the voltage across the energy storage capacitor, v_{Ce} , and the SPS output voltage v_{GD} . The start-up voltage of the prototype V_{start} is preset at $100V$. As shown in Fig 4-9(a), when v_{Ce} increases from zero at time instant t_0 , the MOSFET gate signal is prohibited and the MOSFET is turned off. When the voltage v_{Ce} reaches V_{start} at the time instant t_1 , the MOSFET is enabled, and the energy stored in the capacitor C_e starts to be transferred to the output capacitor C_o of the SPS, leading to a voltage drop on v_{Ce} and an increase in v_{GD} . The variations of v_{Ce} cannot disable the operating of the MOSFET until v_{Ce} falls below V_{min} at time instant t_2 as shown in Fig. 4-9 (b). Therefore, the performance of the hysteresis band is verified experimentally.

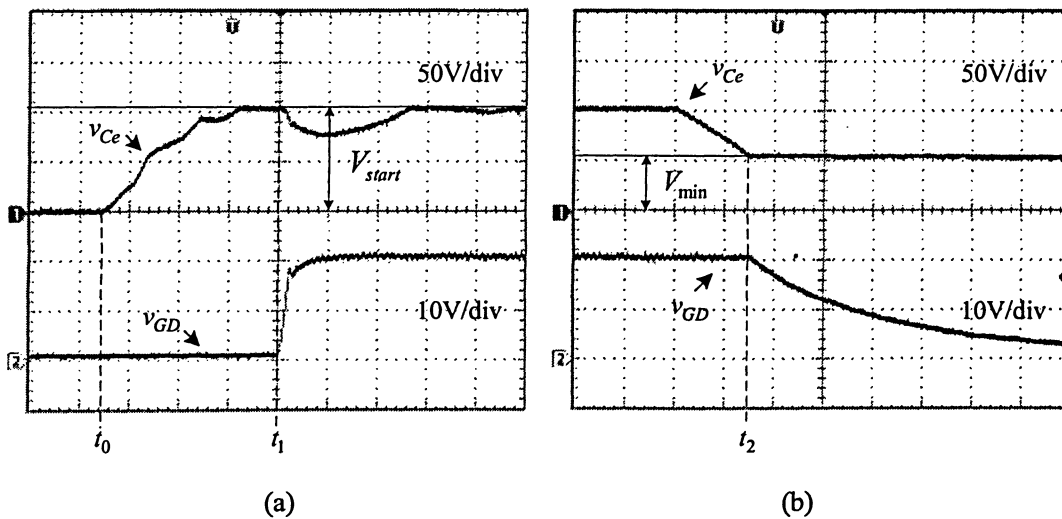


Fig. 4-9 Waveforms for the hysteresis band of the MOSFET controller

In summary, the proposed SPS has the following features.

- **Low insulation requirement.** Since the snubber circuit is at the same potential as the GCT device, the insulation level of the self-powered supply is reduced from a few thousand volts to a couple of hundreds volts.
- **Low manufacturing cost and physical size.** Due to its low insulation requirement, the proposed SPS does not require a high-voltage isolation transformer, leading to a significant reduction of the manufacturing cost and physical size.
- **No influence to the operation of the RC snubber circuit.** Since the energy storage capacitor C_e is significantly larger than (≥ 100 times) the snubber capacitor C_s , and the maximum voltage on C_e is limited to a couple of hundred Volts, the SPS does not interfere with the operation of the snubber circuit.
- **High output power.** By adjusting the maximum input voltage V_{\max} and the energy storage capacitance C_e , the SPS could achieve a high output power. The laboratory SPS prototype can provide 80W for the GCT gate drivers.
- **Good output voltage regulation.** The SPS is controlled by a closed loop with a high switching frequency of 132kHz. The output voltage regulation can reach $\pm 0.5\%$. The SPS does not need any dummy loads when it operates under light load conditions.
- **Wide operation range.** The supply can operate stably and reliably in discontinuous and continuous current modes with different load conditions.

4.4 Summary

This chapter focuses on two major experimental tasks. One task is to verify the proposed simulation model for GCT gate drivers. The gate driver simulation model has two salient features: 1) it is a general model that can be used for any GCT devices, and 2) it is also a simplified model that can be easily integrated to other simulation programs. The experiments for this task were conducted on a 4160V current source drive.

The second experimental task is to verify the performance of the proposed self-powered supply (SPS) for GCT gate driver. A laboratory prototype SPS of 60W was designed and built. Various experiments were carried out for the SPS operating under different conditions.

It can be concluded that the proposed SPS can satisfactorily operate under the rated and no load conditions with both continuous and discontinuous current modes. The self-powered supply features low manufacturing cost, high output power (60W), and small physical size.

CHAPTER 5

CONCLUSIONS

The commercial dc power supply for the GCT gate driver is an expensive device since the supply has to withstand a medium voltage (MV) of a few thousand volts between its output and input. To meet the insulation requirement, the dc power supply normally employs a high-voltage isolation transformer to provide an electrical insulation between the supply and system ground, which makes the power supply costly and bulky. To solve the problem, a novel self-powered supply (SPS) is proposed in this thesis for the GCT gate driver, where the SPS transfers energy from the snubber circuit of the GCT device and provides a regulated dc voltage of 20V for the GCT gate driver. Since the snubber circuit is at the same potential as the GCT device, the insulation level of the self-powered supply is reduced from a few thousand volts to a couple of hundred volts, leading to a significant cost reduction.

The technical challenges of the self-powered supply for GCT gate drivers come from the special gating requirements for GCTs, such as large gating currents with high di/dt , no effect on snubber circuit operation, and regulated output voltages. Therefore, the SPS techniques proposed in literature for GTO and SCR devices are not suitable for GCTs.

The proposed SPS is composed of two parts: Converter 1 and Converter 2. Converter 1 is used to transfer energy from the snubber circuit to the energy storage capacitor without affecting the operation of the snubber circuit. In Converter 2, a flyback dc-dc converter regulates the variable output voltage of the Converter 1 into a stable dc voltage of 20V for the GCT gate driver. The flyback transformer of the converter provides a low-voltage insulation between the GCT gate driver and the snubber circuit. Due to the high switching frequency and the close loop

control, the output voltage of Convert 2 meets the critical requirements of the GCT gate driver.

The main contributions of this thesis are as follows:

- 1) **A novel self-powered supply for the GCT gate driver is developed.** The proposed SPS can transfer sufficient energy from the snubber circuit to power the GCT gate driver. It can also provide a low-voltage isolation between the snubber circuit and the GCT gate driver. Therefore, the high-voltage isolation transformer commonly used in commercial GCT gate driver power supplies can be eliminated, leading to a significant reduction in both manufacturing cost and physical size.
- 2) **The maximum power requirement for the GCT gate driver is fulfilled with no influence on the snubber circuit.** A novel method for the maximum power transfer from GCT snubber circuits to the SPS is proposed and implemented. The proposed SPS can provide an output power up to $60W$ for most commercial GCTs, and in the meanwhile, it has little impact on the operation of the snubber circuit.
- 3) **Effective simulation models are developed.** Simulation models are developed to investigate the performance of the proposed SPS. To improve the efficiency of the simulation, a simplified model for GCT gate drivers is proposed. This model is valid for any GCT gate drivers.
- 4) **A prototype of the proposed SPS is implemented.** To verify the performance of the proposed SPS, a laboratory prototype has been implemented and tested. The experimental results have verified that the proposed SPS can satisfactorily meet the technical requirements for GCT gate drivers.

- 5) **Design guidance is provided.** The design guidance for the proposed SPS is provided. The relationship between the maximum output power and supply parameters, such as the values of the maximum SPS input voltage, energy storage capacitor, snubber capacitor, and the utility supply voltage, is provided and given in a graphical format.

Future Work

This thesis focuses on the development of a self-powered supply for current source rectifier. When the rectifier system is powered up, the utility voltages will be automatically applied to GCT devices, from which the proposed SPS can obtain energy from the GCT snubber circuit.

It is suggested that the possibility of applying the proposed SPS technique to current source inverters to be investigated, where the dc link voltage is not constant, and may start from zero during power-up.

APPENDIX

A. Typical Parameters of A Medium-voltage Current Source Rectifier

| | |
|-----------------------------|--|
| Rated Line Voltage | 4160V |
| Rated Power | 0.4MVA |
| Switching Pattern | Selective Harmonic Elimination (SHE) |
| Harmonic to be eliminated | 5 th , 7 th and 11 th |
| Switching Frequency | 420Hz |
| Total line inductance L_s | 0.1pu |
| Filter capacitor C_f | 0.5pu |
| dc current inductance L_d | 0.87pu |
| dc load resistance R_d | 1.2pu |
| Snubber Capacitor | 0.1 μ F |
| Snubber Resistor | 10 Ω |

B. Specifications for Commercial GCT Gate Drivers

| GCT Gate Driver | | Repetitive peak off-state voltage $V_{DRM}(V)$ | Repetitive controllable on-state current $I_{TQRM}(A)$ | Gate Unit Voltage $V_{GDC}(V)$ | Gate Unit Consumption $P_{Gin}(W)$ |
|-----------------|-----------------|--|---|--------------------------------------|--|
| ABB | 5SHX 04D4502 | 4500 | 340 | 20 ± 0.5 | 11 |
| | 5SHX 06F6004 | 5500 | 520 | 20 ± 0.5 | 16 |
| MITSUBISHI | GCU04AA-1 30 | 6500 | 400 | 20 ± 1 | 20 |
| | GCU08BA-1 30 | 6500 | 800 | 20 ± 1 | 35 |
| | GCU15CA-1 30 | 6500 | 1500 | 20 ± 1 | 50 |

The above table shows the specifications of a number of GCT devices manufactured by ABB and Mitsubishi. The supply voltage for GCT gate drivers is typically rated at $20V$ with a tolerance of $\pm 0.5V$ and its power rating is from $10W$ to $60W$.

C. GCT Gate Driver

The GCT gate driver is a special design, which integrates the GCT device. The GCT is turned on or off by adding a positive or negative voltage between the gate and cathode terminal of the GCT device.

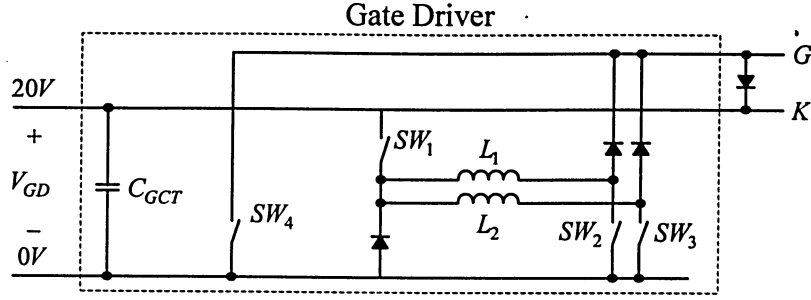


Fig. A-1 Circuit diagram of GCT gate driver

Fig. A-1 shows a simplified circuit diagram of the GCT gate driver [15]. When the turn-off signal is applied, the switch SW_4 is on, and meanwhile the switches SW_1 , SW_2 , and SW_3 are all off. The gate-cathode terminal is kept negative biased ($V_{GK} = -20V$). The current flowing through the cathode of the GCT (K) is then commutated into the gate terminal of the GCT (G). This novel switching mode is characterized by an extremely fast commutation of the cathode current to the gate whereby the cathode emitter is turned off before the voltage across the anode and the cathode of the GCT rises. To achieve this performance, the whole cathode current is commutated to the gate within less than $1\mu s$ [19, 22]. During this process, a higher di/dt normally greater than $3000A/\mu s$ is produced, and a large amount of energy is dissipated.

When the turn-on signal is applied, the switches SW_1 , SW_2 , and SW_3 are all on, and meanwhile the switch SW_4 is off. The pulse current is built up in chokes L_1 and L_2 . Once the necessary amplitude is attained, the choke current is commutated into the gate terminal in two steps by turning off switch SW_2 first, and then SW_3 . While the turn-on pulse is executed, it only needs a small on-state gate current to keep the GCT conducting [24].

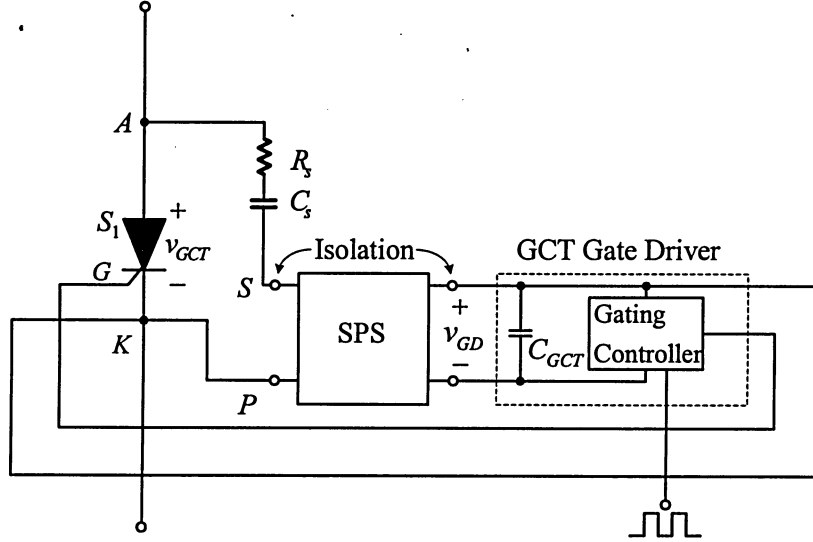


Fig. A-2 Block diagram of SPS and GCT gate driver

Fig. A-2 shows the block diagram of the self-powered supply (SPS) and the GCT gate driver. The positive output terminal of the SPS is connected with the cathode of the GCT, K and the negative input terminal of the SPS, P via the GCT gate driver. And hence, the two input terminals of SPS, S and P will be connected together if no isolation is provided between the snubber circuit and the GCT gate driver. To ensure the power supply working properly, the SPS provides the isolation by its internal step-down transformer as shown in Fig. 2-2.

D. Schematic of the Self-powered Supply Prototype

Fig. A-3 Schematic of the self-powered supply Prototype.

64

REFERENCES

- [1] Bin Wu, 'High Power Converter Systems', Wiley - IEEE Press & John Wiley, March 2006, ISBN: 0-4717-3171-4.
- [2] Li Chun, Jiang Qirong, Xu Jianxin, 'Investigation of Voltage Regulation Stability of Static Synchronous Compensator in Power System', Power Engineering Society Winter Meeting, Vol.4, No.4, pp. 2642 – 2647, January 2000.
- [3] Nielsen J.G, Newman M., Nielsen, H., Blaabjerg F., 'Control and Testing of A Dynamic Voltage Restorer (DVR) at Medium Voltage Level', Power Electronics, IEEE Transactions, Vol.9, No.3, pp. 806 – 817, May 2004.
- [4] P.K. Steimer, H.E. Gruning, et al, 'IGCT – A New Emerging Technology for High Power Low Cost Inverters,' IEEE Industry Application Magazine, pp. 12 -18, July/August, 1999.
- [5] H.M. Stillman, 'IGCTs – Megawatt Power Switches for Medium Voltage Applications,' ABB Review, No. 3, pp. 12-17, 1997.
- [6] S. Eicher, S. Bernet, et al, 'The 10 kV IGCT - A New Device for Medium Voltage Drives' IEEE Industry Applications Conference, pp.2859 -2865, 2000.
- [7] N. Zargari, Y. Xiao and B. Wu, 'A Near Unity Input Displacement Factor PWM Rectifier For Medium Voltage CSI Based AC Drives,' IEEE Industry Applications Magazine, Vol.5, No.4, pp.19-25,1999.
- [8] Ned Mohan, Tore M. Undeland, William P. Robbins, "Power Electronics: Converters, Applications, and Design, 3rd Edition", Wiley - IEEE Press & John Wiley, September 2003, ISBN: 0-471-22693-9.
- [9] Dusan M. Raonic, "SCR Self-Supplied Gate Driver for Medium-Voltage Application with Capacitor as storage Element ", IEEE Transaction on Industry Applications, Vol.36, No.1, pp.212-216, January/February 2000.
- [10] Dusan M. Raonic, "SCR Self Supplied Gate Driver for Medium Voltage Application with

Capacitor as Storage Element”, IEEE Industry Applications Conference, Vol.2, No.1, pp.1168-1173, October 1998.

- [11] Dusan Raonic , Dave MacLennan, Didier Rouaud, “Some Experience with SCR’s Self Powered Gate Driver System for Medium Voltage Solid State Starter” IEEE Canadian Conference on Electrical and Computer Engineering Conference (CCECE 97), Vol.2, No.1, pp.556-559, May 1997.
- [12] Hiromichi Tai, “Gate Power Supply Circuit”, U.S. patent 5483192, January 1996.
- [13] David R. Deam, “Apparatus and Method for Utilizing a Snubber Capacitor to Power a Silicon-controlled Rectifier Gate Trigger Circuit”, U.S. patent 6396672B1, May 2002.
- [14] Dusan Raonic, David S. MacLennan, Didier G. Rouaud, “Self-powered Gate Driver Board”, U.S. patent 5796599, August 1998.
- [15] Navid R. Zargari, Bin Wu, Weiqian Hu, “Self-powered Supply for GCT Gate Driver” U.S. patent application, submitted to International Property office, Rockwell Automation, Wisconsin, March 2006.
- [16] Weiqian Hu, Bin Wu, Navid R. Zargari, ‘A Novel Self-Powered Supply for GCT Gate Driver’, IEEE Applied Power Electronics Conference and Exposition (APEC), March 2007.
- [17] Abraham I. Pressman, ‘Switching Power Supply Design’, McGraw-Hill, July 1998, ISBN: 0-07-052236-7.
- [18] Power Integrations, ‘TOPSwitch Flyback Design Methodology Application Note AN-16’, November 2005.
- [19] B. Degard, R. Ernst, "Applying IGCT Gate Units", ABB Application Note 5SYA 2031-1, December 2002.
- [20] N. Zargari, S.C. Rizzo, et al, ‘A New Current Source Converter Using a Symmetric Gate Commutated Thyristor (SGCT),’ IEEE Trans. on Industry Application, Vol.37, No.3, pp.896-902, 2001.
- [21] Navid R. Zargari, Steven C. Rizzo, Yuan Xiao, Hideo Iwamoto, Katsumi Satoh, John F.

Donlon, "A New Current-Source Converter Using a Symmetric Gate-Commutated Thyristor (SGCT)", IEEE Transactions on Industry Applications, Vol.37, No.3, pp.896-903, May/June 2001.

- [22] K. Satoh, M. Yamamoto, T. Nakagawa, and K. Kawakami, "A New High Power Device GCT (Gate Commutated Turn-off) Thyristors," in Conf. Rec. EPE'97, pp.70–75, 1997.
- [23] Eric Carroll, Sven Klaka, Stefan Linder, "Integrated Gate-Commutated Thyristors: A New Approach to High Power Electronics", IGCT Press Conference, May 1997.
- [24] MITSUBISHI, "Mitsubishi GCT Thyristor Unit GCU15CA-130", March 2004.
- [25] Power Integrations, "TOP242-250 TOPswitch-GX Family Application Notes", November 2005.
- [26] Power Integrations, "TOPSwitch Power Supply Design Techniques for EMI and Safety Application Note AN-15", November 2005.